Heliophysics Senior Review 2017

The Reuven Ramaty
High Energy Solar Spectroscopic Imager
(RHESSI)

Samuel Krucker, Principal Investigator

Brian Dennis, Mission Scientist

Albert Shih, Deputy Mission Scientist

Manfred Bester, Director of Operations

Table of Contents

EXECUTIVE SUMMARY

RHESSI has provided diagnostic observations of high-energy processes in solar flares for over 15 years since its launch in February 2002. These observations address the key Heliophysics goal of understanding the fundamental processes of energy release and particle acceleration in solar eruptions, both flares and coronal mass ejections (CMEs).

RHESSI is designed for imaging spectroscopy of hard X-ray (HXR) and gamma-ray continua emitted by energetic electrons, and gamma-ray lines produced by energetic ions. The single instrument makes imaging and spectroscopy measurements with a few arcsecond angular resolution and one- to a few- keV energy resolution at energies from soft X-rays to gamma-rays (3 keV to 17 MeV). **No other current observatory has this ability to provide imaging spectroscopy of the energetic particles that carry such a predominant part of the released energy in a flare.** (The Spectrometer Telescope for Imaging X-rays (STIX) on the European Solar Orbiter will provide X-ray imaging spectroscopy of flares following launch in late 2018 or early 2019.) Thus, **RHESSI remains an essential component of the Heliophysics System Observatory (HSO)**. Interpretation of data from RHESSI, especially in conjunction with data from other instruments and predictions of theoretical flare models, forms a key part of "*developing a comprehensive scientific understanding of the fundamental physical processes that control our space environment and that influence our Earth's atmosphere.*"

Considering the age of the RHESSI mission, the spacecraft and instrument continue to operate well. The mission has no expendables and reentry is not predicted to occur until December 2022, with the earliest predication been October 2021. The slowly rising detector temperature resulting from the gradually decreasing cryocooler efficiency is of concern. The need to minimize the temperature increase has led us to operate only two of the nine detectors during times of low solar activity. When there is enhanced activity and during joint observing campaigns with other space and ground-based observatories, we have been turning on additional detectors for optimum coverage.

Over 114,000 events are included in the RHESSI Flare List. Almost 22,000 of them have detectable emission above 12 keV, 610 above 50 keV, 199 above 100 keV, and 42 above 300 keV; 27 events show gamma-ray line emission. All the data and the analysis software have been made immediately available to the scientific community. This has resulted in **over 1,000 refereed papers** published to date that utilize RHESSI observations with more than **200 in the last two years alone since the Senior Review in 2015 and an average citation rate of** well over **4,000 citations per year.**

The value of RHESSI observations has been greatly enhanced by improved complementary observations compared with those available during the first half of RHESSI's operational lifetime. Groundbreaking observations of thermal plasmas, magnetic fields, and heliospheric effects are now being provided on a regular basis by instruments on the Solar Dynamics Observatory (SDO), Hinode, STEREO, the Interface Region Imaging Spectrograph (IRIS), Fermi, and other components of the HSO. In the same way, **the value of future RHESSI observations is will be greatly enhanced by upcoming missions such as Solar Probe Plus and Solar Orbiter, but also by ground-based observatories in the optical and the radio wavelength range.** Of greatest interest are joint observations with the Expanded Owens Valley Solar Array (EOVSA) that provides highly complementary diagnostics of flare-accelerated electrons at a level that has never been accessible before. Despite the low solar activity expected for the period covered by this proposal, RHESSI will provide groundbreaking new findings from joint observations with these newly available observatories.

1 SCIENCE AND SCIENCE IMPLEMENTATION

Fifteen years of near-continuous operation have brought RHESSI into a new era of observational success. Launched near the peak of Solar Cycle 23 in February 2002, RHESSI has provided its unique X-ray and gamma-ray imaging spectroscopy (3 keV to 17 MeV) for well over a complete 11-year cycle. (See Section 2 for more details on RHESSI's capabilities.) During Cycle 24 starting in 2009, the value of RHESSI observations has been greatly enhanced by measurements from an unprecedented array of new space missions and ground-based facilities.

1.1 Prioritized Science Goals (PSGs) – Progress to Date

In the 2015 Senior Review proposal, RHESSI's overall science goal of understanding solar flare energy release and particle acceleration was broken down into the following four major elements plus two additional components derived from RHESSI's serendipitous optical and non-solar capabilities:

(1) Evolution of solar eruptive events (SEEs),
(2) Acceleration of electrons,
(3) Acceleration of ions
(4) Origin of thermal plasma.
(5) Optical Sun
(6) X-ray and gamma-ray sources of both terrestrial and astrophysical origin

In this section, we outline the progress that has been made in the last two years in each of these six areas. In Section 1.2 we discuss how new observations made with RHESSI in the coming years will remain important in addressing these key science goals.

RHESSI hard X-ray observations have shown that the flare-accelerated electrons and ions are both intimately related to the magnetic restructuring associated with solar eruptive events (SEEs), defined as flares with associated coronal mass ejections (CMEs). They have confirmed that together these particles contain a large fraction of the total released energy (Emslie et al. 2012, Aschwanden et al. 2015, 2016a, 2016b, 2017). Additionally, RHESSI's high sensitivity down to ~3 keV has allowed the highest temperature flare plasma to be located and characterized. There have also been systematic studies of coronal HXR sources, both those with little or no detectable footpoint emission (Guo et al. 2013) and those only visible to RHESSI when the bright flare footpoints are occulted by the limb (Effenberger et al. 2017). **As a result of these studies, fundamental new information has been obtained on the energy release, electron and ion acceleration, and plasma heating processes in flares.**

RHESSI has also made fundamental discoveries in other areas of solar, terrestrial, and astrophysical studies. RHESSI's solar aspect system (SAS) has provided the best global measurements of the large-scale structure of the solar photosphere (e.g., the solar oblateness) ever obtained, opening up new areas of research that relate to the nature of the solar cycle now and in the future. RHESSI's discovery that Terrestrial Gamma-ray Flashes (TGFs) commonly extend up to >~20 MeV has revitalized the study of these lightning-associated high-energy phenomena. RHESSI also provides measurements of astrophysical high-energy phenomena such as magnetars and cosmic gamma-ray bursts.

One of the greatest strengths of the RHESSI observations lies in their complementarity with data sets from other instruments in the HSO. The relationship between RHESSI and SDO, STEREO, Hinode, and now IRIS, is symbiotic. We note also the beginning of solar observations with MinXSS, NuSTAR, EOVSA, and ALMA. These other sources provide information never before available to aid in the interpretation of RHESSI high-energy observations.

At present, we are past the maximum phase of Solar Cycle 24, and RHESSI has been detecting an average of ~5 flares per day at energies above 12 keV since 2011. Useful average rates of about one flare per day above 3 keV should persist through 2019. For the first time, we

will have a full complement of multi-platform solar and heliospheric measurements throughout a solar cycle and into a second solar minimum. Historical records of activity show that major energetic events can occur at almost any phase of the solar cycle, such as the four X-class flares in December 2006. Furthermore, aspects of solar activity revealed in flare/microflare occurrence patterns may help us to understand the cycle itself.

1.1.1 Science Goal 1 – Evolution of Solar Eruptive Events

A primary goal of heliophysics is to understand the origin and evolution of solar flares and coronal mass ejections, and the relationship between them. It is now well established that magnetic reconnection in the corona plays a central role in the physics of solar eruptive events (SEEs), in which a flare and a CME are observed together. Progress in this science goal has been very good in the last two years thanks to new joint observations by RHESSI, SDO/AIA, and various radio observatories that are showing more clearly than ever before how these events are driven and how they evolve.

1.1.1.1 *Global Energy Budget*

An expanded new project has been undertaken on the global energetics of 400 M- and X-class flares that occurred since the launch of the SDO in 2010. It uses all available observations of these events from AIA, HMI, and RHESSI, with newly developed data analysis techniques for the calculation of energies of all components except for the accelerated ions (Aschwanden et al, 2014, 2015, 2016a, b, and 2017). The range of values found for some components are remarkably different from those found by Emslie et al. (2012) as indicated in Figure 1. For example, the estimated free magnetic energies are significantly lower as the result of the more detailed analysis of the magnetic field data compared to the very rough estimate used by Emslie et al. (2012). More problematic is the much higher values for the energy in flare electrons found by Aschwanden et al. (2016a) as a result of using the warm, thick-target model of Kontar et al. (2015) with a mean temperature of 8.6 MK. This gives a mean low-energy cutoff energy of 6.2 ± 1.6 keV, significantly lower than the values of ~20 keV used by Emslie et al. (2012), who used the cold thick-target model. While this may be correct in some events, it clearly over-estimates the energy in electrons in other cases where the values obtained of up to 3×10^{33} ergs greatly exceed the highest total bolometric energy ever recorded of 3×10^{32} erg that is included in the Emslie et al. (2012) events.

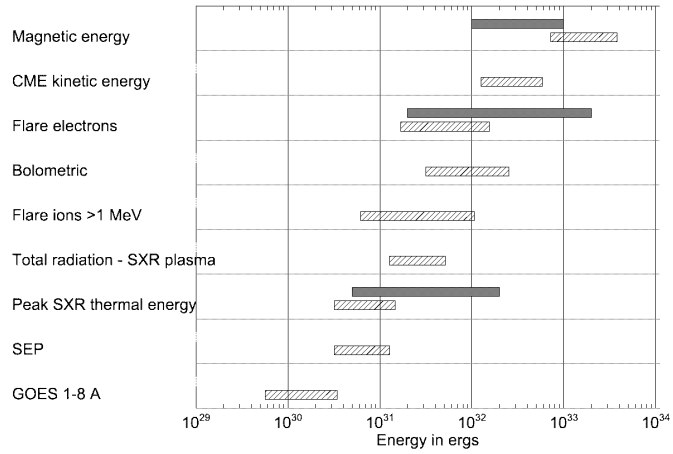

Figure 1. Bar chart showing the logarithmic ranges of energies reported by Emslie et al. (2012, hatched boxes) and by Aschwanden et al. (2016a, black boxes).

While details of the global energy budget remain controversial, it is clear that a large fraction of the released magnetic energy is manifested as accelerated electrons and ions, and that there is a general equipartition, to within an order of magnitude, between the flare and the CME energies. However, the goal of achieving "closure" between the estimated magnetic free energy dissipated in an event and the sum of the energies in all the different products remains elusive. More work is needed to test the energy closure in each of the analyzed flares and to scrutinize the validity of the warm thick-target model, the magnetic origin of CMEs, and to find upper limits on alternative energy dissipation processes such as direct heating, wave heating, and ion acceleration.

1.1.1.2 *Quiescent Filament Eruptions*

Although quiescent filament eruptions occur outside active regions, they sometimes have the properties of SEEs but with generally weak X-ray flares. X-ray images have not previously been available to determine the location of flares that were temporally associated with filament eruptions. It is possible that any such flare is triggered sympathetically in a nearby active region when the filament erupts, and this would be consistent with the study by Hannah et al. (2011) that did not find any X-ray microflares outside of active regions using RHESSI. However, the RHESSI observation of a compact X-ray flare co-spatial with the expanding western ribbon of a long, erupting quiescent filament and CME demonstrates that this was not the case for this event (Holman & Foord, 2015). The X-ray flare was located near a small, magnetically strong, dipolar region below the filament, but was not in a numbered NOAA active region.

This discovery of X-ray flare emission in direct association with a quiescent filament eruption points to a new diagnostic of the hottest plasma that is likely to be associated with the area of most rapid energy release and the trigger of the eruption. Therefore, analysis of more events such as this should provide new insights into the physical conditions associated with the onset of filament and SEE eruptions and the conditions required for bright flares.

1.1.1.3 *HXR Emissions from CMEs*

Statistical studies of RHESSI observations have shown that flare-accelerated non-thermal electrons are injected upward from the acceleration site into the escaping CME core in all eruptive flares analyzed (e.g., Krucker et al. 2017a). Nevertheless, such events can rarely be observed with RHESSI because of the relatively low density of the CME core and the usual presence of intense chromospheric footpoint sources. These types of sources are therefore best seen in highly occulted flares where the main flare emissions occur behind the solar disk as in Figure 2.

Quantitative comparisons derived from joint SDO/AIA and RHESSI data show that electrons injected into the CME are responsible for heating the core of the ejected CME material by collisions (Glesener et al. 2013, Krucker et al. 2017a). Hence, the previously unexplained heating observed in CME material as it moves outward (e.g., Landi et al. 2010) is due to flare-accelerated non-thermal electrons as they lose their energy by collisions, and heat the CME core.

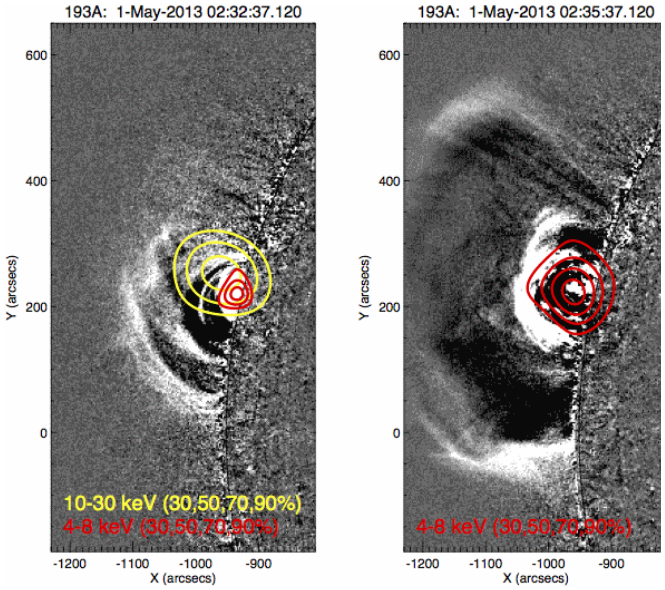

Figure 2. RHESSI and SDO/AIA 193Å imaging of an escaping CME with the actual flare site being occulted behind the solar limb. The two frames, taken 3 minutes apart, show the CME in EUV running-difference images overlaid with RHESSI X-ray contours. The red contours show thermal emission from the hot CME core, while the yellow contours give the location of non-thermal electrons seen only during the initial phase (Krucker et al. 2017a).

1.1.2 Science Goal 2 – Flare-accelerated Electrons

Solar flares have shown us that impulsive energy release in a magnetized cosmic plasma drastically accelerates electrons. Questions critical to understanding flares include: When, where, and how are electrons accelerated, and what happens to them afterwards? How can such a large fraction of the energy released in flares appear as energetic non-thermal electrons? Possible explanations draw both on

fundamental theoretical properties of the reconnection process and on the observed properties of electron acceleration in reconnection events observed *in situ* in the solar wind, deep in the Earth's magnetotail, and in laboratory plasmas. RHESSI provides crucial information to address this question through observations of the HXR emission (predominantly electron-ion bremsstrahlung) that the accelerated non-thermal electrons produce when they interact with the ambient medium. RHESSI's X-ray imaging spectroscopy capability allows electron distributions in space and energy to be determined as functions of time during a flare.

Significant progress has been made on this science goal in the last two years thanks to new observations from RHESSI, IRIS, SDO, and various radio observatories. Improved spectral analysis tools have also been introduced that incorporate various additional items that had not previously been included such as a warm thick target (Kontar et al. 2015), return currents (Alaoui & Holman 2017), and non-uniform ionization (Su et al. 2011) providing a more realistic insight into electron acceleration, propagation, and total energy.

1.1.2.1 ***Electron Propagation***

Alaoui & Holman (2017) have included the effect of return currents on the interpretation of RHESSI hard X-ray spectra. They applied a simple return-current model (Holman 2012) to a selection of flares with strong spectral breaks and relatively flat spectra below the break. The return current stabilizes the accelerated electrons as they stream toward the chromosphere and resupplies electrons to the acceleration region. The induced electric field that drives the return current also extracts energy from (decelerates) the streaming electrons and leads to Joule heating. This model fits the spectral data in most cases, and is also consistent with RHESSI and related imaging data. The results suggest that the resistivity of the flare plasma is somewhat greater than the classical (Spitzer) value. They also provide constraints on the injected electron flux density and low-energy cutoff.

1.1.2.2 ***Use of Coordinated X-ray and Radio Observations***

Radio observations are an ideal complement to RHESSI HXR flare observations since they provide physically distinct perspectives on energetic electrons, hot plasma, and the magnetic field. Combining X-ray with different wavelength radio observations leads to important new diagnostics.

Microwave observations allow electron spatial, spectral, and temporal distributions to be derived independently from HXRs (e.g. Nita et al. 2015). An example of joint RHESSI and Nobeyama Radio Heliograph observations is shown in Figure 3. Since the HXRs are density-weighted bremsstrahlung emission, while microwaves are magnetic-field-weighted gyrosynchrotron emission potentially from the same population of electrons, coronal magnetic field strengths during flares can, in principle, be derived at different positions along the flare loop. Estimates of the coronal magnetic field strength and its evolution during a flare are crucial for evaluating flare energy budgets, for understanding particle acceleration and transport, and for investigating the processes involved in CME initiation.

Decimeter-wave and meter-wave observations generally show coherent emission from energetic electrons associated with escaping electron beams, plasmoid ejecta, and CMEs (e.g., Reid et al. 2014). Coherent radio bursts emitted at around the local plasma frequency provide complementary diagnostics to RHESSI HXR observations to study electron acceleration associated with flares.

Following the completion of the extension to the Karl G. Jansky Very Large Array (VLA), we can for the first time, image decametric emission above 500 MHz at high spectral (1 MHz) and temporal (50 ms) resolution. Figure 4, adapted from Chen et al. (2015), shows combined VLA and RHESSI observations of a termination shock in the outflow region of a magnetic reconnection current sheet. These observations strongly suggest that the reconnection termination shock drives the electron acceleration, at least in part.

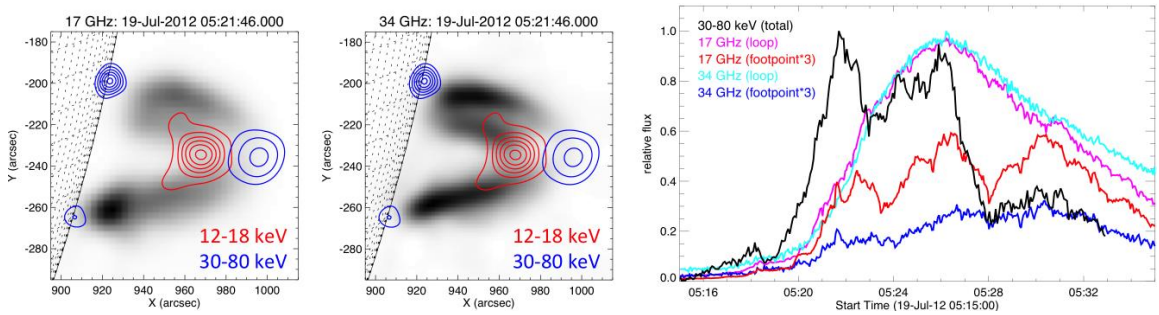

Figure 3. Example of combined HXR and microwave observations from RHESSI and Nobeyama. Left and center: Microwave images at 17 and 34 GHz are shown with RHESSI contours in the thermal (12–18 keV) and non-thermal (30–80 keV) range. Right: Time evolution in HXRs and microwaves. Note the good correspondence of the footpoint time profiles in both wavelength ranges produced by precipitating electrons, while trapped electrons radiate in microwaves from the loop with a gradual time profile. It is currently not understood why the above-the-loop-top HXR source is not seen in microwaves.

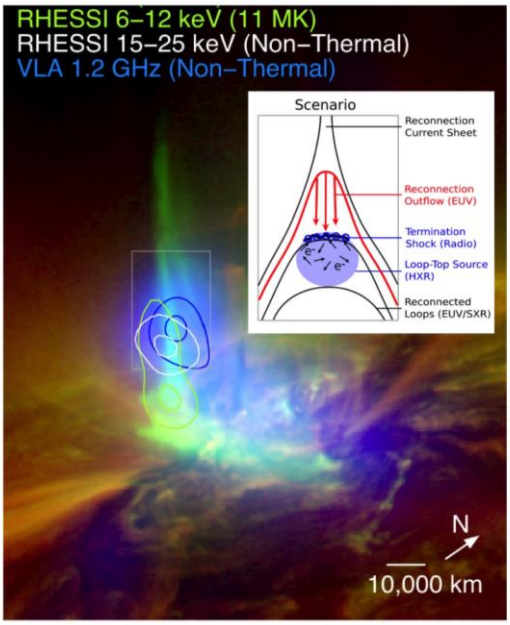

Figure 4. An eruptive flare seen in this combined AIA image at 131 Å (green) and 171 Å (red) overlaid with VLA radio and RHESSI X-ray contours. Near co-spatial radio and HXR non-thermal sources are observed near the top of hot flaring loops at ~10 MK. The insert shows the scenario of emission processes near the termination shock. Radio spikes are emitted as accelerated electrons impinge on density fluctuations at the shock (blue circles). These electrons also produce a HXR source (blue shadowed region).

1.1.2.3 *Simultaneous multi-instrument X-ray and EUV spectral fitting*

Observations at EUV wavelengths, in particular from SDO/AIA, provide important constraints for the low-energy part of the electron spectrum to which RHESSI is not sensitive. Since the bulk of the energy is contained in this part of the spectrum, properly constraining it is not only crucial for observations of the acceleration region as described above, but also significantly reduces the uncertainties in total flare energy calculations. Motorina & Kontar (2015) and Battaglia et al. (2015a) developed a method that allows for true simultaneous fitting of RHESSI spectra in conjunction with SDO/AIA observations with a kappa distribution. The authors demonstrate that, particularly in the case of single-source or occulted events, the method results in a considerable reduction of inferred low-energy electrons when compared with extrapolations from fits to RHESSI data only. This results in a factor of five reduction in total energy compared with traditional, single-instrument analysis. Figure 5 shows the mean electron spectrum inferred from analyzing AIA data and RHESSI spectra individually in comparison with the spectrum inferred from the new method.

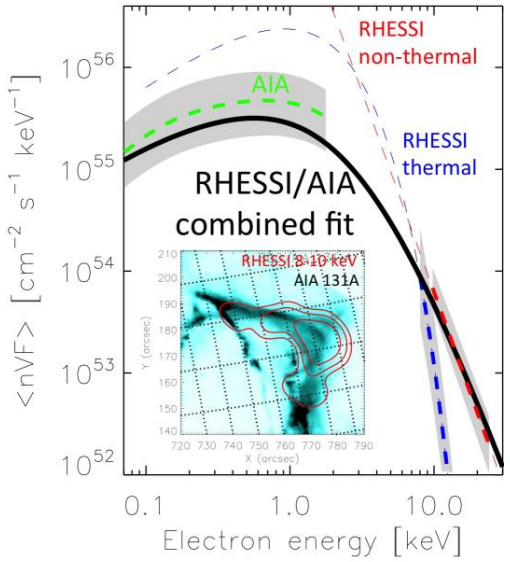

Figure 5. Mean electron flux spectra inferred by Battaglia et al. (2015) using RHESSI and AIA observations of the single-loop flare (shown in inserted AIA image with overlaid RHESSI contours). The colored dashed lines give the spectra derived from the two instruments over the energy ranges for which they could be deduced and extrapolated into the unobservable range (thin lines). The thick black line gives the overall spectrum when the two data sets are fitted together using the method developed by Motorina & Kontar (2015).

1.1.3 Science Goal 3 – Flare-accelerated Ions

There can be comparable energy content in flare-accelerated ions and flare-accelerated electrons (e.g., Emslie et al. 2012), and thus understanding the role of ions in flares is critical. The nuclear de-excitation lines, the positron-annihilation line at 511 keV, and the neutron-capture line at 2.223 MeV in flares reflect the composition, spectrum, and angular distribution of the accelerated ions, and also the density and composition of the solar atmosphere in which the ions interact. RHESSI provides measurements of all of these gamma-ray spectral features for the largest and most energetic solar flares, and it has observed the neutron-capture line in tens of flares.

Progress in this science goal over the last two years continues despite being limited by the absence of extreme gamma-ray line flares. The largest gamma-ray flare observed by RHESSI in this cycle so far was the X4.9 flare on 2014 February 25 (SOL2014-02-25). While it was not sufficiently intense in the 2.2 MeV neutron-capture line to allow for statistically useful imaging in that line, images can be made of the gamma-ray continuum up to 1.5 MeV as shown in Figure 6 revealing where relativistic electrons are depositing their energy. Relativistic electrons are known to have a striking correlation with ~30 MeV/nucleon ions (Shih et al. 2009), and RHESSI provides key location information not available from any other observatory.

Exciting new advances have been made on two types of gamma-ray events: over-the-limb events with gamma-ray sources covering a large area on the visible disk, and the events discovered with the Large Area Telescope (LAT) on Fermi with >100 MeV gamma-ray emission lasting for several hours. In addition, a new method (Torre, 2015) allows proton spectra to be determined from the gamma-ray data without any prior assumptions about the distribution. This is unlike the standard forward-fitting method that is usually used where the spectral form is assumed to be a power law.

1.1.3.1 *Location and Extent of Gamma-ray Source(s)*

One of the most astonishing gamma-ray flares of the current solar cycle was SOL2014-09-01 occurring in an active region on the back side of the Sun (Ackermann et al. 2017). Fermi/LAT detected >100 MeV emission from accelerated ions that managed to reach the photosphere on the front side of the solar disk and produce gamma-ray photons through the pion-decay process. RHESSI observations reveal that the accelerated electrons seen in HXRs are coming from an extended coronal source as shown in Figure 7. The observations show that the >10 keV X-ray emission came from a source with an angular extent greater than the 3 arcminutes of RHESSI's coarsest subcollimator. The off-axis location of the source allowed us to estimate a source extent of about a solar radius, implying electron trapping in extended coronal structures (Krucker et al.

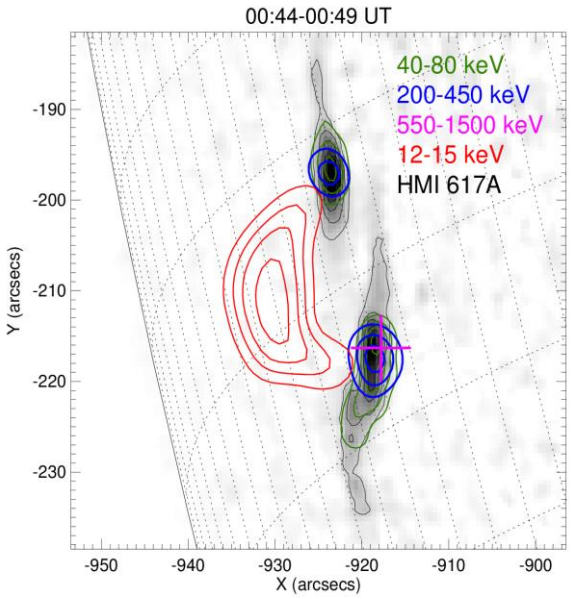

Figure 6. HMI reversed intensity white-light image of the X4.9 flare on 2014 February 25, overlaid with RHESSI color-coded contours showing X-ray and gamma-ray sources in the indicated energy ranges. The centroid of the gamma-ray source at energies up to 1.5 MeV (shown as the pink cross) reveals where relativistic electrons are depositing their energy.

2017a). Complementary observations by RHESSI and Fermi reveal how ions and electrons are accelerated, trapped, and transported as the solar eruptive event evolves to very large spatial scales.

1.1.3.2 *Fermi/LAT Events*

Fermi/LAT has detected >~100 MeV emission from tens of SEEs since its launch in 2008 (Share et al. 2017). Many of these events fall into the category of long-duration gamma-ray flares (LDGRFs), with emission persisting for many hours following the impulsive phase of the flare. While this emission is likely from the decay of pions produced by >300 MeV protons accelerated by the SEE, the time and site of the acceleration remain unknown.

RHESSI observations complement the LAT observations by providing imaging and spectroscopy for HXR and gamma-ray emission during the impulsive phase of the flare, and upper limits for the sometimes hours afterwards when LAT still detects >100 MeV gamma rays. While Fermi/GBM spans a similar energy range to RHESSI, it does not provide any imaging information.

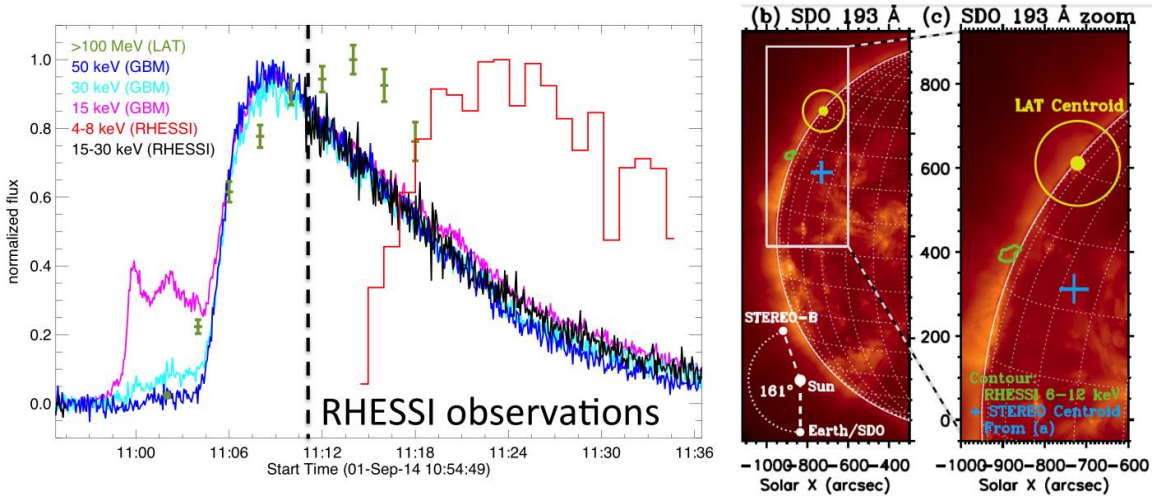

Figure 7. Time evolution and source location of the occulted flare SOL2014-09-01 as seen by RHESSI and Fermi LAT and GBM (adapted from Ackermann et al. 2017). Left: LAT observed an impulsive increase at >100 MeV and GBM observed a HXR burst with a smooth profile decaying for up to 30 minutes. RHESSI covered the decay and provided imaging information. Right: The >100 MeV emission is likely to be coming from near the limb as suggested by the LAT centroid location; the blue cross indicates the location of the occulted AR as it would be seen through the Sun. RHESSI reveals thermal, 6–12 keV emission (green contour) at the limb above the occulted AR, but the >20 keV emission also detected by RHESSI is coming from an extended source (not shown in figure) with a size of about half a solar diameter.

1.1.4 Science Goal 4 – Flare-heated Plasma

The hot plasma in flares appears simultaneously with flare-accelerated particles (the Neupert effect). Characterizing the temperatures and locations of flare-heated plasma reveals the partition between direct heating and collisional losses of the accelerated particles. RHESSI is sensitive to the hottest plasmas with temperatures above ~10 MK and is also uniquely capable of determining the energy of flare-accelerated particles and *where* that energy is deposited.

Significant progress has been made in achieving this science goal over the last two years as the result of extensive coverage of events jointly observed by RHESSI and by UV and EUV instruments on SDO, Hinode, and IRIS and by ground-based optical observatories. The new results cover thermal emissions from all altitudes in the flaring solar atmosphere. Together with the energy of the accelerated electrons determined from the RHESSI HXR observations, they provide quantitative information on the origin, location, and magnitude of the heating for comparison with the predictions of ongoing theoretical and modeling efforts.

1.1.4.1 *Complementary IRIS and RHESSI Observations*

With the launch of the IRIS mission, there is a new sub-arcsecond diagnostic tool to study the response of the energy input into flare ribbons by flare-accelerated electrons as deduced from RHESSI observations. The X1 flare SOL2014-03-29 gave us an ideal set of observations with the IRIS slit crossing a HXR footpoint source during the impulsive phase (Figure 8). IRIS detected, for the first time from space, hydrogen recombination UV radiation resulting from the flare-accelerated electrons measured by RHESSI (Kleint et al. 2016).

Quantitative analysis of the same area of the flare ribbon reveals that the energy input by electrons deduced from RHESSI data is of the same order as the radiative losses inferred from IRIS in combination with other observatories. The bulk of the energy of flare-accelerated electrons heats chromospheric plasma only to low (~10,000 K) temperatures, producing high luminosity in

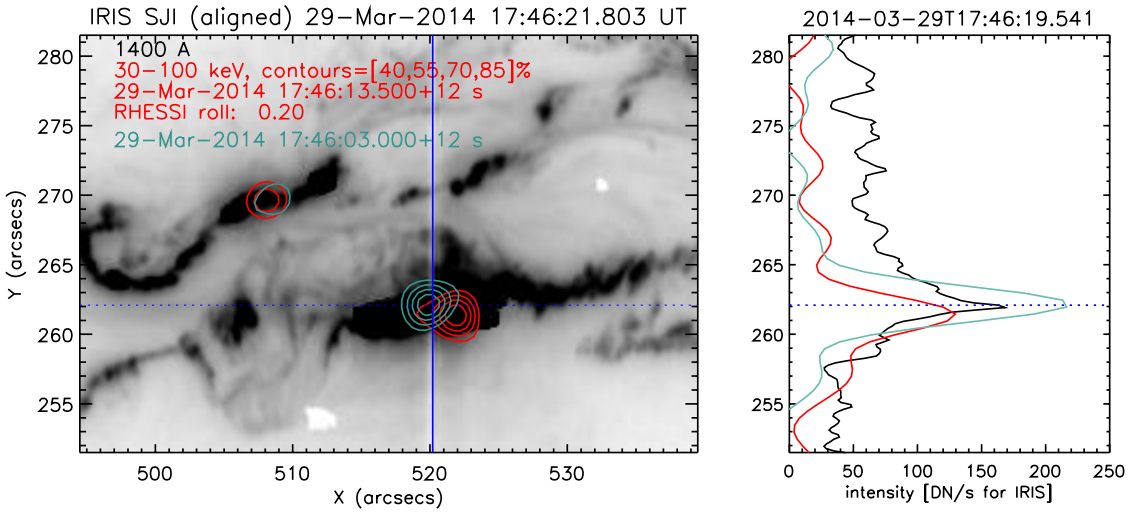

Figure 8. Combined RHESSI and IRIS observations of flare ribbons: HXR contours (30-100 keV) are overlaid on an IRIS slitjaw image (adapted from Kleint et al. 2016). Red RHESSI contours are simultaneous to the IRIS image; green RHESSI contours were recorded 10 s earlier. In this rare example, the IRIS spectrograph slit (blue solid line) passed directly through the HXR source, enabling us to directly compare the relative timing and energies of non-thermal electrons and the continuum emission. The right panel shows an intensity cut along the spectrograph slit. The intensity maxima of early-RHESSI (green) and continuum emission (black) indicate that the continuum emission is excited nearly instantaneously after the electron bombardment with a delay of no more than 15 s, which will have implications on future modeling efforts.

the optical-IR range (e.g. Kleint et al. 2016, Kowalski et al. 2015), at least for the few events studied in detail. For all these studies, RHESSI plays a key role in providing quantitative information on the location, duration, and strength of the energy input into the chromosphere by flare-accelerated electrons.

IRIS also provides measurements of hot (~10 MK) plasma through the FeXXI line (Battaglia et al. 2015b) revealing upflows of hot plasma from the flare ribbons and hot downflows from the reconnection region deduced from RHESSI imaging. Comparing these upflows with the location of HXR footpoint emission allows us to test the standard flare picture, where evaporation is caused by flare-accelerated electrons precipitating into the chromosphere. Alternatively, conductive evaporation or direct photospheric heating are alternative mechanisms. Results of the X-class flare of SOL2014-03-29 reveal that some locations with strong upflows indeed match the HXR footpoints, but with a rather puzzling time lag of about 1 minute (Battaglia et al. 2015b). Other locations with equally strong upflows, however, are not detected in HXRs, indicating that a different mechanism, possibly thermal conduction, drives the evaporation at these locations.

1.1.4.2 *Complementary HMI and RHESSI Observations*

Two recently published statistical studies (Kuhar et al. 2017, Huang 2016) that include all flares above GOES M5 level with simultaneous RHESSI and HMI observations have revealed that there is a clear correlation, both spatial and temporal, between the white-light (WL) intensity seen by HMI and the HXR flux observed by RHESSI (Figure 9). This indicates that WL production is a general feature of solar flares, but detection of WL emission for smaller flares becomes more difficult because of the relatively large and continual fluctuations at optical wavelengths.

New RHESSI and SDO results establish that HXR and WL emissions from flare ribbons are co-spatial in ***all three dimensions*** (Krucker et al. 2015). Most surprisingly, both emissions originated from the same very low altitudes above the photosphere, at only a few 100 (±150) km in one event. Such low altitudes strongly restrict the parameter space for the standard thick-target beam model. Only very low ambient densities within the flare footpoints can reproduce such altitudes, especially if the HXR-producing electrons are only weakly beamed as suggested by spectral observations. To explain such low HXR source altitudes, Varady et al. (2014) proposed local re-acceleration within chromospheric ribbons. For such a case, the secondary acceleration

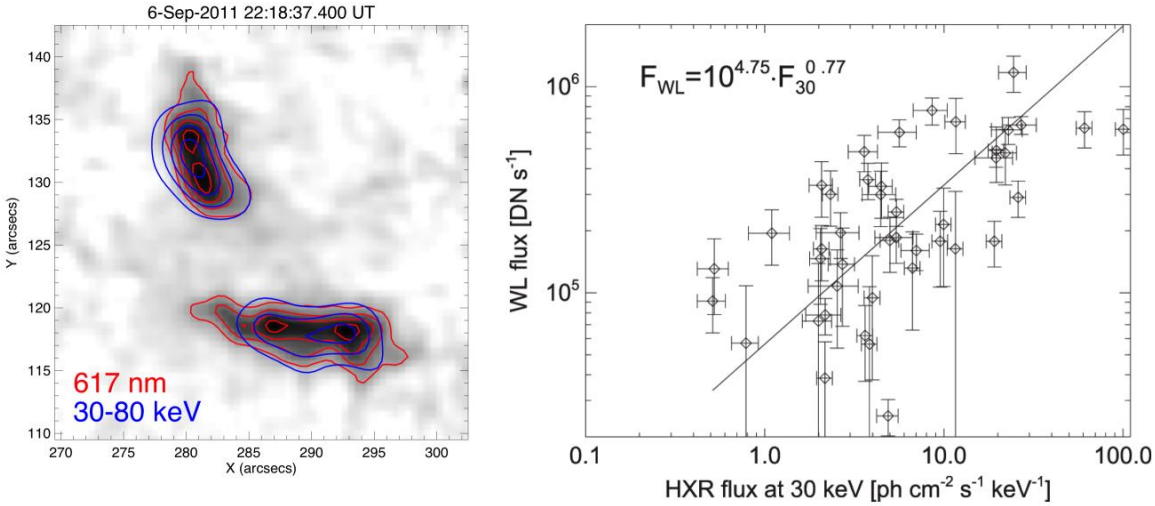

Figure 9. RHESSI and SDO/HMI observations of flare ribbons. Left: The image shows the background-subtracted HMI 617 nm image with the darker areas indicating enhanced emission. The contours give the RHESSI 30–80 keV hard X-ray emission in blue, and the HMI flux in red. Note the excellent spatial correlation of the HXR and WL emission. Right: Scatter plot of the WL and HXR flux for all jointly observed flares (from Kuhar et al. 2016).

in the chromosphere allows the electrons to reach lower altitudes compared to the standard thick-target model. However, the nature of the secondary acceleration lacks observational evidence, and its source of energy is problematic.

1.1.4.3 *Infrared to mm-wave continuum*

The Halloween flares of 2003 provided the unexpected, and still unexplained, discovery of bright flare emission at 1.56 μm, the "opacity minimum" region of the solar atmosphere (Xu et al. 2004). Now we have related observations at 5 μm and 10 μm (Penn et al. 2016). Figure 10 shows the first IR flare observations from the McMath telescope at Kitt Peak National Observatory with the IR emission matching the X-ray impulsive phase in both space and time. The IR and HXR observations are consistent with the picture that the flare-accelerated electrons heat and ionize the chromosphere to produce thermal IR radiation. The IR flux increases during the times of the HXR bursts with a close match between the IR time derivative and the HXR time profile. This exciting development inspires our proposed efforts to understand RHESSI observations in the context of these new ground-based IR and submm-mm wave (ALMA) observations.

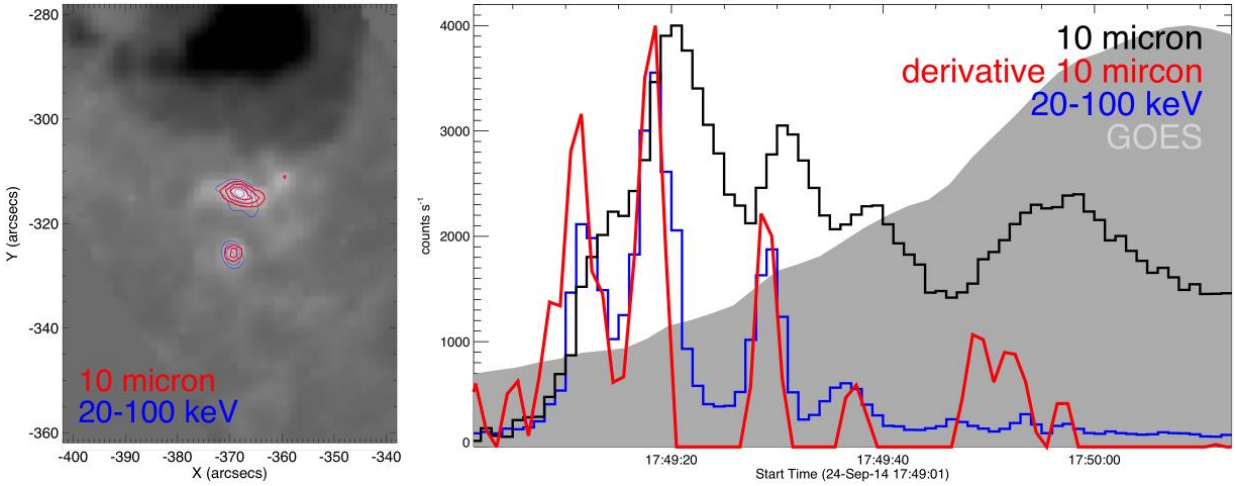

Figure 10. Infrared observations of SOL2014-09-24 (C7.0) at 10 μm from the McMath telescope at NSO Kitt Peak. Note the close agreement of the IR and RHESSI HXR footpoint sources, as well as the close temporal correlation with the HXR time evolution matching closely the time derivitate of the 10 micron flux (adapted from Penn et al. 2016).

1.1.4.4 *Flare ribbons: hot chromospheric response*

Collisional heating by flare-accelerated electrons is not only responsible for optical and IR radiation, but also for heating flare ribbons to MK temperatures making them visible in EUV and SXRs. However, even for modest flares, the ribbons are so bright that AIA observations of them are generally heavily saturated making quantitative analysis difficult. The newly available de-saturation algorithm developed by the RHESSI team now allows us to properly study the EUV counterparts of the HXR footpoints (Schwartz et al. 2015). Figure 11 shows the result of the de-saturation, revealing a close match between the heated ribbons seen in EUV and the location of precipitating electrons as seen in HXRs. From the de-saturated AIA images at different wavelengths, the differential emission measure distribution can be reconstructed revealing hot plasma in footpoints at temperatures up to 10 MK. However, this is well below the 30 MK temperature of the main flare loop seen by RHESSI in the corona for this flare indicating that 'evaporation' of hot plasma from the chromospheric ribbons alone cannot be responsible for creating the hot flare loop seen by RHESSI. Hence, direct heating by the energy release process must be responsible for the highest temperature in flare loops.

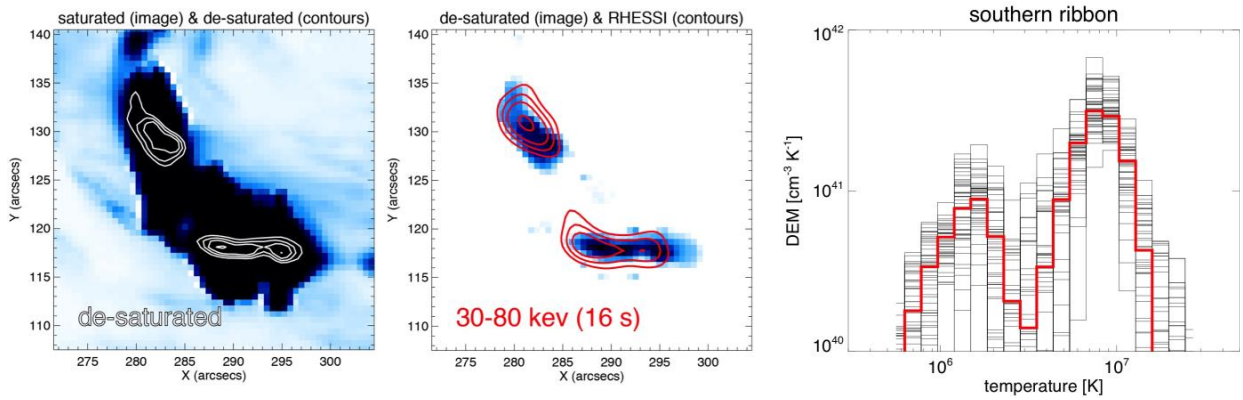

Figure 11. Example of an AIA image at 2011 Sep 6, 22:18:38UT, showing flare ribbons de-saturated using the algorithm described in Schwartz et al. (2015). Left: saturated AIA 131 Å image of the flare ribbon with white contours showing the result of applying the desaturation algorithm. Center: de-saturated image with RHESSI 30–80 keV sources shown by the red contours. Right: derived differential emission measure (DEM) of the southern ribbon from the desaturated AIA EUV images in multiple wavelength bands (from Krucker et al. 2017b).

1.1.4.5 *Computational Models*

Numerical codes that simulate the evolution of flare plasma depend on RHESSI data to deduce the heating function within the plasma. The codes are used to predict the radiation from the solar atmosphere heated by the flare-accelerated electrons as they propagate down from the corona. They take the flare-accelerated electron spectra derived from RHESSI HXR observations and predict the thermal emissions for comparison with GOES, EVE, SDO, Hinode, IRIS, and RHESSI observations at many different wavelengths (e.g. Allred et al. 2015). By minimizing the residuals between the predicted and observed intensities and light curves, the models can be constrained and fine-tuned.

As an example, Figure 12 shows X-ray source motions in a flare loop observed by RHESSI in three energy bands (dashed curves). Reep et al., (2016a) modeled these source motions with simulations incorporating either in situ deposition of energy in the corona or heating by non-thermal electrons. Only the simulations with heating by non-thermal electrons were able to adequately reproduce the location of the sources and their time evolution for this flare.

Kennedy et al. (2015) used a simulation with a single flare loop to model the time evolution of the emission measure, temperature, and density of flare plasma deduced from GOES, EVE, and RHESSI data for a flare on 9 March 2011. The results from their simulation did not match the evolution of these data well. Successes and similar difficulties were found in comparing observations with predictions for an event on 25 September 2011 observed by the EIS instrument on Hinode (Doschek et al. 2015). Reep et al. (2016b) got better agreement with the data for a flare on 2014 November 19, including spectral line redshifts, using a multi-threaded model. They found the average time between the heating of the individual strands to be less than 10 s. Rubio da Costa et al. (2016) modeled spectral line emission from a flare on 2014 March 29 obtained with IBIS and IRIS. RHESSI data were used to determine the heating function. Their multi-threaded model was able to closely reproduce spectral line profiles.

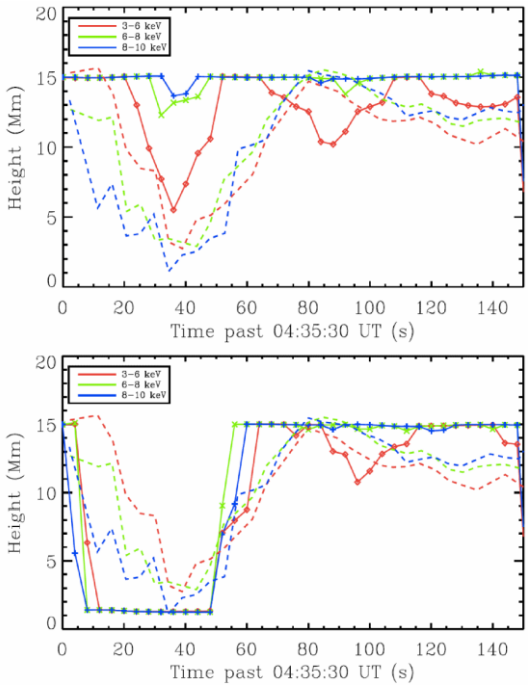

Figure 12. Comparison of RHESSI measurements of X-ray source height in three energy bands as a function of time (dashed lines) with numerical simulations (solid lines) for a flare on 2002 Nov 28. The top panel is for a thermal model with *in situ* heating at the top of the loop, and the bottom panel is for heating by energetic electrons (adapted from Reep et al. 2016a).

Work is ongoing to refine the simulations and resolve the discrepancies by adapting different parameters such as the duration of heating by non-thermal particles on individual field lines, as well as by increasing the total energy of the non-thermal electrons by lowering the cutoff energy below the upper limit provided by RHESSI.

1.1.4.6 *Thermal Coronal Plasma*

RHESSI is also uniquely capable of characterizing the so-called "super-hot" (>~30 MK) flare plasma (see Caspi et al. 2014a). Not only does RHESSI provide high-resolution spectroscopy of such plasmas that are otherwise inaccessible to currently operating SXR observatories, RHESSI can compare the spatial locations and evolution of super-hot plasma against the relatively cooler ~10–20 MK plasma. RHESSI's imaging approach enables the use of visibility-based analysis techniques to produce images at different ***temperatures*** rather than merely in different energy bands (Caspi et al. 2015). This newly developed technique has been demonstrated and validated for isothermal components, and can be applied to more complex spectral components.

1.1.5 Science Goal 5 – Global Structure of the Photosphere

Because of its requirement for sub-arcsecond aspect information, RHESSI incorporates correspondingly precise tools for image reconstruction and alignment, including the solar aspect system. This requirement resulted in an additional capability for RHESSI to study the Sun at visible wavelengths with a rapidly rotating telescope in space, a method never previously employed. The rapid rotation of RHESSI (~15 rpm) around the solar direction provides a crucial advantage, since it allows for deconvolution of instrumental image distortion and greatly simplifies flat-field corrections, temperature corrections, and other factors that make photometry and astrometry difficult at the parts-per-million level.

Fivian et al. (2008) used these capabilities to obtain the most precise measurement of the solar oblateness, defined as the excess of the equatorial radius over the polar radius. Using only three months of the available data at an intermediate state of solar activity and screening against contamination by magnetic features at the limb, they reported a solar oblateness value of (8.01 ± 0.14) milli-arcseconds. This is consistent with the Dicke estimate of 7.98 milli-arcseconds expected from the rotation of the Sun taken as being constant in cylinders around the rotational axis. It exceeds in precision all other measurements (both space and ground), including the more recent ones from SDO (Kuhn et al. 2012) and PICARD (Irbah et al. 2014).

Recent work has concentrated on revising and refining the masking of magnetically contaminated optical data by external EUV proxies (Fivian et al., 2016) and also on determining the pole-to-equator temperature gradient with new emphasis on the estimate of the uncertainty of such measurements (Fivian et al. 2017). Our best value of pole-to-equator temperature difference of ~0.05 K is an order of magnitude smaller than previously reported (see Rast et al. 2008).

1.1.6 Science Goal 6 – Nonsolar Objectives

1.1.6.1 *Terrestrial Gamma-Ray Flashes (TGFs)*

Terrestrial gamma-ray flashes (TGFs), millisecond pulses of gamma radiation from lightning, have become a very active field of research worldwide, thanks in large part to RHESSI observations over the past decade. Most recently, two groups (Ostgaard et al. 2015, Smith et al. 2016) have been using RHESSI's passages over known lightning flashes in the radio to search for faint TGFs and even weaker gamma-ray emission in a targeted fashion. In the former paper, an additional (but small) population of TGFs was discovered, about a factor of 2 fainter than the faintest that could be identified previously. In the latter paper, we examined the summed gamma-ray signal from all lightning that RHESSI overflew, and demonstrated that this total emission is remarkably small, meaning that the total number of weak TGFs – including even those that could never be identified individually by any method – is also very small. In other words, no more than ~1% of lightning produces a TGF of more than 10^{-4} of the magnitude of a typical one observed from space. This is good news in terms of pilot/passenger safety from TGF radiation, an issue that has been receiving more attention over the past few years.

In other recent work, RHESSI have been used to show that in the minority of TGFs where there are two gamma-ray peaks, it is the second that produces the brightest radio signal (Mezentsev et al. 2016). This may have implications, which have not yet been explored, for the (still unknown) TGF formation mechanism. RHESSI was also used, along with the Fermi satellite, for a rare stereoscopic view of three TGFs (Gjesteland et al. 2017).

1.1.6.2 *Cosmic Gamma-Ray Bursts (GRBs)*

Thanks to its broad energy range and wide field of view (>2π sr), RHESSI has made valuable contributions to the study of cosmic gamma-ray bursts (GRBs). These energetic transients have peak energies ranging from tens to hundreds of keV, and RHESSI continues to be a useful tool for continuum spectroscopy of GRBs (e.g., Bellm 2010; Ripa et al. 2012). RHESSI has detected over 1100 GRBs to date. RHESSI is also assisting with the prompt localization of GRBs (136 to date, K. Hurley, private communication) as part of the Interplanetary Network (IPN), which localizes GRBs by triangulation, comparing the time profiles seen by spacecraft in different parts of the solar system. Prompt localization enables rapid follow-up by telescopes at all wavelengths from radio to X-rays, providing data on both the source of the explosion and the environment in the host galaxy.

RHESSI has also observed ~70 magnetar bursts, including the notable 2004 event from SGR 1806-20. A recent study (Huppenkothen et al. 2014) made use of RHESSI's high time resolution to argue for the presence of magnetic coupling between the crust and the core of the magnetar. With the discovery of gravitational radiation by LIGO, the search has begun for simultaneous gamma-ray and gravitational-wave transients, which would be a clear signature of a compact binary coalescence. The IPN and RHESSI are actively engaged in this exciting project, which would open a new astrophysical window.

1.2 How the Prioritized Science Goals will be achieved

RHESSI remains a key complement to the HSO, uniquely providing information on the hottest plasma and the energetically important electrons and ions. **No other instrument can provide**

both the location and spectra of the highest temperature plasma and the flare-accelerated electrons and ions. Thus, the primary requirement for achieving our Prioritized Science Goals (PSGs) is for RHESSI to continue to provide X-ray and gamma-ray imaging spectroscopy during the declining phase of the current solar cycle.

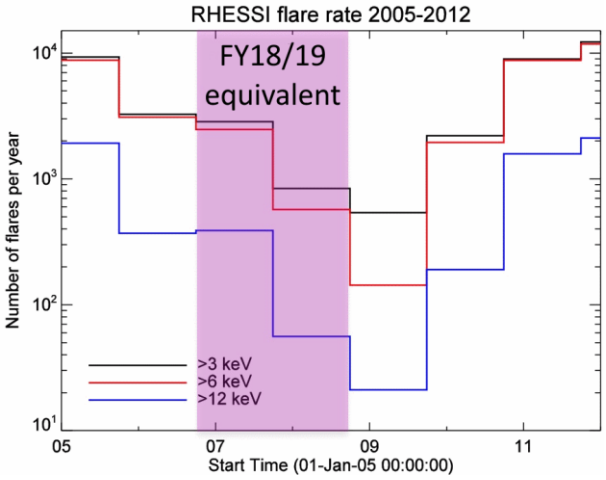

Figure 13. Number of flares recorded by RHESSI per fiscal year above the indicated threshold energies through the last solar minimum from 2005 to 2011. The shaded region indicates the equivalent phase of the solar cycle corresponding to FY18 and FY19.

The 2018 to 2019 time interval will have decreasing solar activity as we approach the solar minimum expected in ~2020, so it is prudent to estimate the number of flares RHESSI will detect during this period. This can be accomplished by using the previous solar minimum as a guide when RHESSI was fully operational. Figure 13 shows the number of flares in the RHESSI catalog for the 7 years around the last solar minimum in 2009. Since RHESSI now typically has only two of its nine germanium detectors turned on at a time, we can expect to detect somewhat fewer flares (perhaps down by a factor of ~3) at the time of the next minimum even if the Sun is equally active. Then, using an 11-year solar cycle period, we can expect to detect 2423/3 ≈ 800 events above 6 keV in FY'18 and 563/3 ≈ 190 in FY'19. These estimates are consistent with the numbers of events already detected in FY'16 and the first three months of FY'17.

In addition to the existing HSO space assets, eagerly anticipated new radio capabilities are expected to be available during this same time period, providing invaluable imaging spectroscopy observations over wide frequency ranges. These include several new major facilities including VLA, ALMA, and other new facilities, but **the main new strength lies in the solar-dedicated EOVSA. We have never before had simultaneous microwave and RHESSI hard X-ray imaging spectroscopy, and this is the key to many problems of flare and active-region development.** These two spectral bands show aspects of the same phenomena with distinctly different physical processes. In the past, we have had hints of this capability from the fixed-frequency "slices" of the microwave spectrum, and with EOVSA we will now get the full and detailed spectrum of the radio emission at every point in the image, and at every moment in time. EOVSA is expected to become fully operational in 2017, and we expect that the first few detected C- and M-class events will produce breakthrough observations. Simultaneous EOVSA and RHESSI observations will be even more powerful, with the combination of the two offering far greater insight into the high-energy flare processes than either one separately.

1.2.1 Science Goal 1 – Evolution of Solar Eruptive Events

The occurrence of solar eruptive events has a strong solar-cycle dependence, but we still expect several medium size events to occur in the next years (see Figure 13). Additionally, we will be able to study the newly discovered quiescent eruptions in collaboration with SDO, STEREO, Hinode, and IRIS, in particular their occurrence rate during solar minimum. The main new breakthrough science is anticipated to be joint observations by RHESSI and Solar Probe Plus of impulsive electron events. By tracking the electrons, imaged at the Sun using RHESSI HXR imaging spectroscopy data, through the interplanetary medium using the Type III radio emission, to the *in situ* detection by Solar Probe Plus, we can trace and study the magnetic connectivity from the solar acceleration region to Solar Probe Plus.

1.2.1.1 *Quiescent eruptions and confined events*

RHESSI unexpectedly detected emission from a quiet-Sun filament eruption (Holman & Foord 2015). This expands the dynamic range of events that we can study, so new observations of these eruptions will be sought. Tens of events have been identified in existing data sets, and future observations are planned that include coordinated studies with ground-based and space observatories.

1.2.1.2 *Combined observations with Solar Probe Plus*

Solar Probe Plus (SPP) will be launched in August 2018 and first observations will be available during the second year of the time period proposed here. Of greatest interest for RHESSI are joint observations of electron beams escaping from the Sun as shown schematically in Figure 14 (e.g. Lin 1985). SPP will measure these electrons in situ close to the Sun providing us for the first time with measurements that are only minimally affected by transport effects that tend to wash out the direct signatures of the acceleration mechanism when electrons are observed at 1 AU. Such impulsive electron events come in at least two classes (Krucker et al. 1999) with one class being directly related to the flare site (so-called prompt events), while the second class is observed to be delayed relative the impulsive phase of the flare as the electrons are accelerated at the shock of the eruptive event as it travels outwards from the Sun. For joint observations, prompt events are of great interest as RHESSI can image the associated flare location. This will give us the connectivity of the magnetic field at SPP back to the acceleration site on the Sun. Using statistical results from observations taken at 1 AU (e.g. Wang et al. 2012), the number of events observed during solar minimum may be as low as about 1 event per month. However, the event rate observed by SPP is anticipated to be significantly larger, as SSP at close approach should see much fainter events due to the more intense flux closer to the Sun.

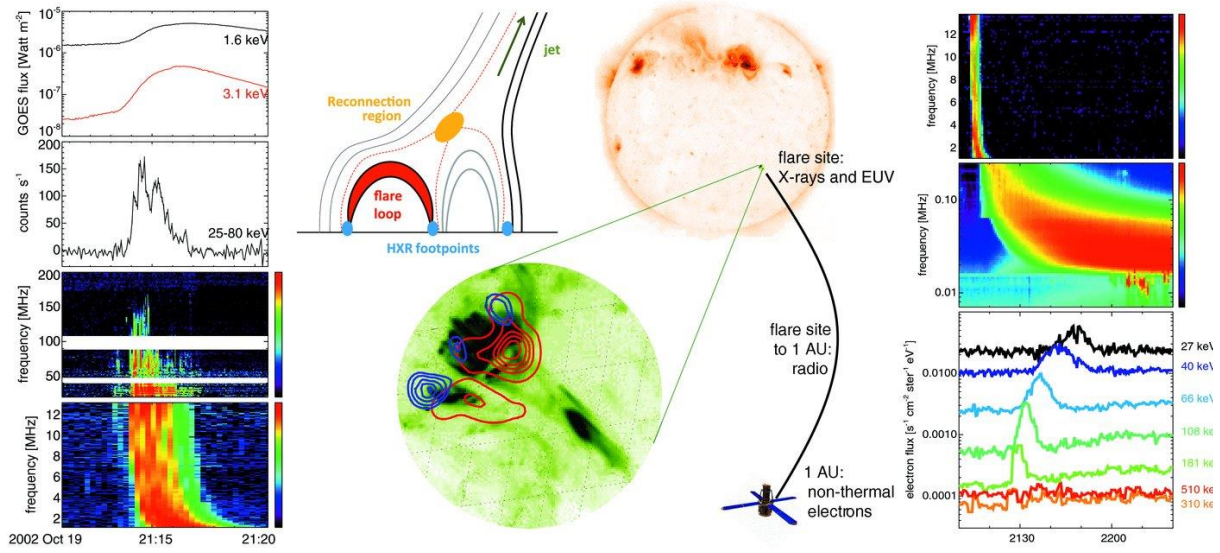

Figure 14. Schematic description of prompt solar energetic electron events. Left and right: time series in soft and hard X-rays, radio waves, and non-thermal electrons seen near 1 AU. These observations track energetic electrons from their acceleration site at the Sun into interplanetary space. Center: hard X-ray and EUV imaging results of the source region are shown together with a schematic of interchange reconnection. The reconnection region, the flare loop, the hard X-ray footpoints, and the jet are labeled. The red dashed lines give the field lines that are currently reconnecting. Previously reconnected field lines are shown in black, while the field lines that will be the next to reconnect are shown in gray.

1.2.2 Science Goal 2 – Flare-accelerated Electrons

1.2.2.1 *Complementary radio observations with EOVSA*

During the past 15 years of RHESSI observations, complementary microwave radio observations were only available with very limited coverage, leaving a large gap in the diagnostics for flare-accelerated electrons. Microwave observations are produced by flare-accelerated electrons that emit gyro-synchrotron radiation as they spiral along magnetic field lines. This provides RHESSI with crucial complementary diagnostics. The only regularly available microwave observations have been from the Nobeyama Radio Heliograph at two single frequencies. For modeling, however, high-resolution imaging spectroscopy observations are essential (e.g. Nita et al. 2015).

The solar-dedicated Expanded Owens Valley Solar Array (EOVSA), observing in the frequency range from 2.5 to 18 GHz, was promised to fill this gap but financial and technical difficulties delayed the project for years. However, EOVSA is now operational and, in January 2017, it has for the first time imaged a microflare in conjunction with RHESSI (see Figure 15). These observations of a GOES B8 flare show that the instrument is working as promised, and we are looking forward to observing many more flares. Even for a moderate C-class flare, the uniqueness of the combined radio and HXR data sets will provide breakthrough science.

1.2.2.2 *Joint observations with the VLA*

The next opportunity for solar VLA observations will be from summer to fall 2018 when the VLA will again be in the D configuration that is favorable for solar observations. These observations will take place around solar minimum, but since VLA observations can be scheduled as targets of opportunity, microflare observations can be guaranteed. As the number of solar VLA flare observations taken so far is limited, with only four published papers to date, any new observations will greatly enhance our collection of jointly observed flares. Microflares are frequently associated with electron beams producing radio type III bursts (e.g. Chen et al. 2013).

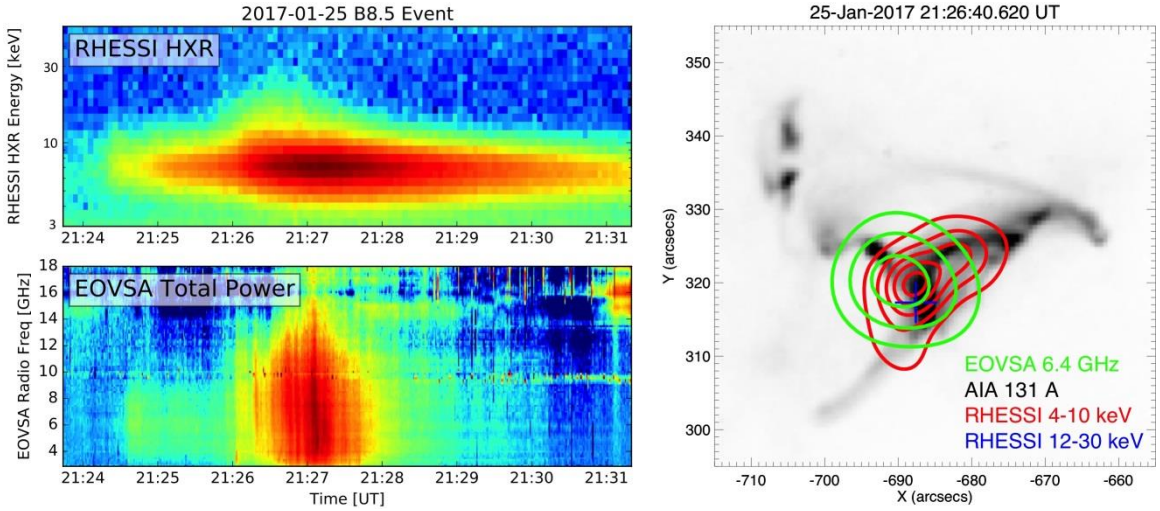

Figure 15. First GOES B8 class flare jointly observed by EOVSA and RHESSI. (Left) The spectral evolution in time is shown for the radio (bottom) and HXR (top) emissions. While both emissions are produced by flare-accelerated electrons, the HXR bremsstrahlung is mainly coming from the dense chromosphere from precipating electrons, while the radio emission is mainly produced by trapped electrons. This difference results in the observed delay in the radio emission. (Right) Imaging observations in HXR and radio reveal a thermal loop (4–10 keV) and gyrosynchrotron emission from trapped electrons within the loop (6.4 GHz). The blue cross gives the centroid location of the HXR emission from non-thermal elecrons precipating primarily at one end of the flare loop.

Tracing these beams through VLA imaging spectroscopy in combination with SDO, Hinode, STEREO, and IRIS observations will reveal magnetic field topology along which accelerated electrons travel in the corona, and if on open field lines, escape the Sun. Of greatest interest are escaping beams that are later observed in interplanetary space by STEREO, WIND, or ACE. RHESSI plays the key role in this investigation showing the location of accelerated electrons in the chromosphere and lower corona.

1.2.2.3 *Joint microflare observations with ALMA*

Atacama Large Millimeter/submillimeter Array (ALMA) will provide comprehensive new views of solar flares, in particular in the lower atmosphere that now seems to be decisively important. ALMA's frequency range from 84 to 950 GHz has not been widely explored, especially not with an instrument with ALMA's outstanding capabilities. In the ALMA frequency range, previous observatories have seen thermal emissions due to flare heating (e.g. Trottet et al. 2011) and synchrotron emission from relativistic electrons (e.g. Gimenez de Castro et al. 2009), but also a currently unidentified component (e.g., Kaufmann et al. 2004) for which none of the proposed theoretical explanations are convincing (Krucker et al. 2013).

With the persisting microflare activity predicted for the next years, conditions are ideal for microflare observations. Unfortunately, the ALMA solar observations made in December 2016 did not catch a microflare because of a pointing error, but future observations will give us a first systematic view of microflares in the sub-THz range, with a large scientific potential. RHESSI HXR observations will provide the spectra and location of the flare-accelerated electrons as an essential input for the interpretation of ALMA microflare observations.

1.2.2.4 *HXR Polarization measurements with POLAR*

POLAR (http://isdc.unige.ch/polar/) is a Compton Polarimeter onboard the Chinese space laboratory Tiangong 2, launched on 15 September 2016. Its primary goal is to measure the polarization of gamma-ray bursts, but it also has the capability of observing solar flares. It was designed and built by a collaboration involving the University of Geneva, the Paul Scherrer Institute in Switzerland, the Institute of High Energy Physics in China, and the National Center for Nuclear Research in Poland. POLAR is equipped with an array of 1600 plastic scintillators to measure linear polarization in the 50–500 keV range. The first POLAR observation of a solar flare is shown in Figure 16.

While thermal bremsstrahlung from flares is expected to be unpolarized, the thick-target beam model predicts strong polarization from the non-thermal footpoint sources depending on the anisotropy of the HXR-producing electrons and the viewing direction to the observer (Leach et al. 1985). Polarization measurements of solar flares have been extremely challenging in the past (e.g. McConnell et al. 2004; Suarez-Garcia et al. 2006) and no definitive results have been obtained to date. POLAR has the capability, for the first time, of measuring the X-ray linear polarization for GOES M- and X-class flares, with an accuracy of better than 5% for the larger events. While RHESSI is not measuring polarization, it is

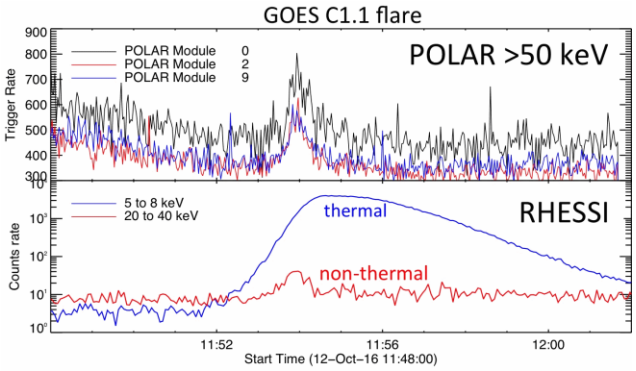

Figure 16. Lightcurves of the first solar flare detected by POLAR on October 12, 2016, and the corresponding RHESSI data. While the C1.1 microflare was clearly detected above 50 keV, the count rate was too low, as expected for such a weak event, to allow for a meaningful polarization measurement, but it shows that POLAR is fully functional.

providing the location of the HXR footpoints and therefore the viewing angle of the flare to the POLAR spacecraft, an essential input for the interpretation of the polarization degree observed by POLAR.

1.2.2.5 *X-ray observations by RHESSI and Solar Orbiter/STIX*

Solar Orbiter is an ESA cornerstone mission with combined remote sensing and *in situ* instruments that will fly as close as 0.28 AU to the Sun. While there are currently some uncertainties about the actual launch date (October 2018 vs. February 2019) and the associated duration of the cruise phase, Solar Orbiter should be operational during the time frame relevant for this proposal. A limiting factor for statistical studies will be the low number of flares expected to be seen during the first years of combined observations. Nevertheless, even for microflares, RHESSI can detect thermal and non-thermal emissions, the two key X-ray components of solar flares.

The primary interest for RHESSI are simultaneous observations with the Spectrometer Telescope for Imaging X-rays (STIX). With the two different viewing angles provided by STIX and RHESSI, two completely new science windows are opening:

(1) Directivity of non-thermal HXR emissions

Depending on the distribution function of the bremsstrahlung-producing electrons, the resulting HXR radiation is emitted with different directional patterns. Thermal bremsstrahlung emission, for example, is produced by isothermal electrons and hence has a uniform pattern. In the standard thick-target beam model, on the other hand, electrons are assumed to be strongly beamed and therefore emit HXRs in a nonuniform pattern with highest emission in the direction of the moving beam. Measuring the directivity therefore provides essential information on flare-accelerated electron distributions (see Figure 17). While previous directivity measurements have been inconclusive due to poor spectral cross-calibration between instruments that were often not solar-dedicated or due to the indirect nature of the observations (e.g., center-to-limb variation studies, albedo studies), combined RHESSI and STIX observations will, for the first time, provide us with systematic measurements of flare directivity.

(2) Occulted vs. on-disk flares

The study of occulted flares has proven fruitful in studying coronal hard X-ray sources, but by their very nature, these observations are not able to simultaneously study both the coronal sources and the much brighter but occulted footpoints. With observations by two spacecraft with different viewing angles such as RHESSI and STIX, both faint coronal and intense footpoint HXR sources can be studied for the same flare (see Figure 18). Such observations will, for the first time, provide us with systematic measurements of coronal and footpoint sources, an important input for testing particle transport models in solar flares.

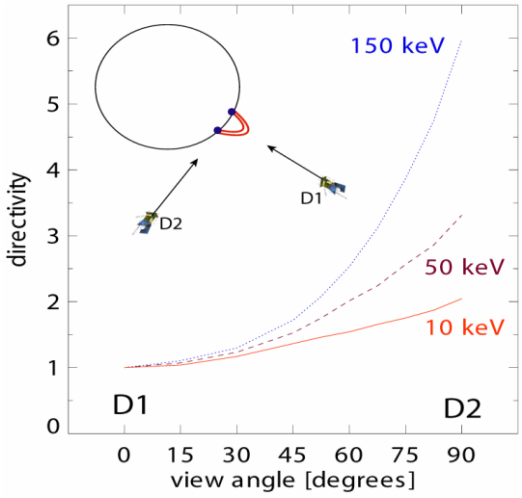

Figure 17. Electron beams penetrating the chromosphere are expected to produce anisotropic emission. The plot shows the relative intensity of the hard X-ray footpoint emission from different view angles with 0º and 90º corresponding to view angles from above (D1) and from the side (D2), respectively.

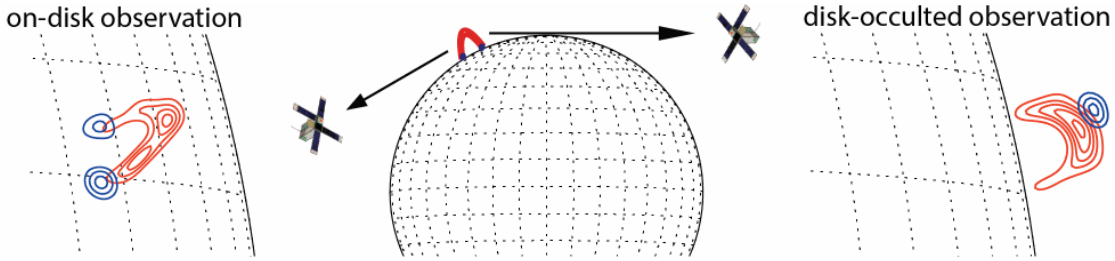

Figure 18. Example of a stereoscopic observation of a flare with RHESSI and STIX taking advantage of the solar disk as an occulter, including (red) thermal and (blue) non-thermal components. One observer (left side, e.g. RHESSI) observes the entire flare, performing imaging spectroscopy of the HXR footpoints. The other observer (right side, e.g. STIX) observes the flare as partly occulted, measuring faint coronal sources including the acceleration region, which is invisible to the unocculted observer in the presence of the bright footpoints because of the limited dynamic range of the instrument.

1.2.3 Science Goal 3 – Flare-accelerated Ions

Fermi/LAT observations of LDGRF ("sustained") gamma-ray emission at very high energies (e.g., Share et al. 2017) complement RHESSI's capabilities and offer a major challenge for identification and interpretation. We will continue the analysis of joint RHESSI/Fermi observations, with the potential for new events that exhibit both impulsive ion acceleration and long-duration >100 MeV emission. In the declining phase of a solar cycle, there can still be extreme solar activity; the period of 2006 Dec 4–18 – less than eleven years ago – included four X-class flares, one of which was associated with the first detection of solar energetic neutral atoms (ENAs) (Mewaldt et al. 2009). Even for smaller events, RHESSI may not be able to directly measure gamma-ray emission, but Fermi/LAT has demonstrated sensitivity to observe >100 MeV emission in even relatively small M-class flares. RHESSI will provide crucial location information on impulsive energy release and accelerated electrons via HXR imaging – not available via Fermi alone – that will be needed to answer the mystery of LDGRF emission.

Existing observations will also be analyzed using the latest techniques to extract *new* information about ions in flares and their evolution. We will extend visibility-based imaging techniques to the gamma-ray range to determine the locations of ion-associated emission, not only of the narrow neutron-capture line, but importantly also the nuclear de-excitation lines and continuum. The typical approach of producing images for energy ranges results in locations that are dominated by the electron-associated bremsstrahlung emission at the same energies as de-excitation emission. Visibilities, however, enable the "subtraction" of the image contribution of electron-associated emission to extract solely the de-excitation emission. An analogous imaging analysis has recently been demonstrated to produce images of different temperature components in the X-ray range (Caspi et al. 2015). The locations of de-excitation emission may be critical information to understanding the apparent spatial separations between ion-associated and electron-associated emission (Hurford et al. 2003, 2006), as well as the enhancement over time in some flares of the relative chromospheric abundances of low-FIP elements.

1.2.4 Science Goal 4 – Flare-heated Plasma

1.2.4.1 *Flare ribbons: energy input and response*

We have a substantial advance in the availability of a large number of complementary data sets provided by IRIS, SDO, Hinode, STEREO, and ground based optical and radio observatories, as outlined in the previous sections. RHESSI data are playing a key role in these studies, as it is the only instrument that provides the energy spectrum and location of the non-thermal electrons.

A challenging part of these coordinated observations is to get observations with the IRIS and Hinode/EIS slit positions intersecting the flare ribbons and the coronal flare region. While we now have a list of ~50 jointly observed IRIS/RHESSI flares, many observations have partially missing coverage and/or sub-optimal slit positions. Additionally, for some flare types we do not have any observations at all. For example, we lack an IRIS/RHESSI flare right at the limb where we could study the radial structure, and hence the altitudes, of the different emissions. It is therefore essential to continue the joint observations even during the current phase of the solar cycle where we mainly expect medium to small flares.

A further improvement of future observations is provided by the coverage with ground-based telescopes. We are planning dedicated campaigns with ground-based observatories such as the newly available GREGOR solar telescope on Tenerife with a 1.5 m mirror, and the New Solar Telescope at Big Bear Solar Observatory (1.6 m mirror), and after 2019, the Daniel K. Inouye Solar Telescope (DKIST) with a 4-m mirror. Never before have such large and powerful optical telescopes been available for solar flare research. Even for microflares, we expect breakthrough new results from such combined observations.

1.2.4.2 *Joint Observations with MinXSS*

The Minature X-ray Solar Spectrometer (MinXSS) CubeSats provide full-Sun SXR spectra from 0.5 to nominally 30 keV (effectively ~10 keV due to limited effective area) with 0.15 keV FWHM spectral resolution. This spectral range complements RHESSI's low-energy (<10 keV) spectra (Figure 19), especially during intense solar flares when the attenuators are engaged and RHESSI loses its response below ~6 keV. MinXSS's resolution, ~5x better than RHESSI's, enables more accurate measurements of the Fe-line complex for temperature and abundance diagnostics (e.g., Phillips et al. 2006). MinXSS also provides access to other important low-FIP elements such as Mg, Si, S, and Ca. MinXSS is sensitive to plasma emission down to ~2 MK, similar to the EUV diagnostics available from SDO/EVE, but has improved sensitivity to hot flare plasma (through continuum and line emission) and no complications from chromospheric line blends. Combining MinXSS and RHESSI spectra is straightforward, and techniques already exist to analyze multi-instrument data to generate DEMs (e.g., Caspi et al. 2014b) to perform solar physics studies sensitive to the full range of hot coronal plasma temperatures, ~2 MK to >50 MK. MinXSS-1 is currently observing, and MinXSS-2 is planned to be launched by September 2017 for a 2-year mission life.

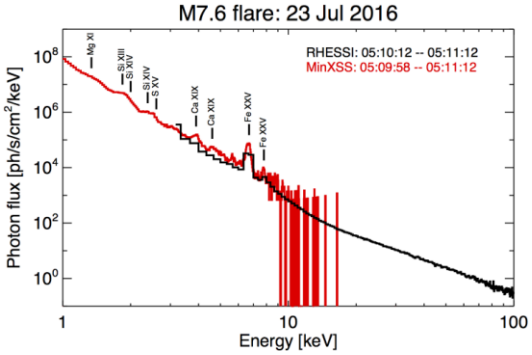

Figure 19. RHESSI and MinXSS-1 observations of the M7.6 flare on 2016 July 23 illustrate how MinXSS extends RHESSI's capability for detailed temperature and abundance diagnostics and how RHESSI provides information – inaccessible to MinXSS – on >~10 MK plasma and non-thermal electrons. The spectral overlap from 3 to 10 keV provides natural cross-calibration between the two instruments.

1.2.4.3 *Joint Observations with NuSTAR*

The Nuclear Spectroscopic Telescope Array *(*NuSTAR*)* is an astrophysics direct-focusing HXR imager aboard a SMEX with 100 times better sensitivity than its predecessors (Harrison et al. 2013). It observes the Sun as an occasional Target of Opportunity. About 30 hours of solar observations have been taken to date (see Grefenstette et al. 2016), but the bulk of solar observation runs are expected to be done during the next several years. NuSTAR is highly sensitive to faint flare-heated plasma and has examined active-region temperature distributions (Hannah et al. 2016), energy release in the late stages of an eruptive event (Kuhar et al. 2017),

HXR flux limits from the quiet Sun (Marsh et al. 2017), and an entirely new range of small microflares (Glesener et al. 2017). However, NuSTAR has some fundamental limitations when observing the Sun, mainly because of throughput limitation, pointing accuracy, and so-called 'ghost rays' (see Grefenstette et al. 2016). Co-observations with RHESSI are therefore crucial for maximizing the solar science that can be accomplished. RHESSI gives precise locations that can be used to co-align NuSTAR flare images, and, with its full-Sun coverage, can pinpoint positions of ghost-ray sources outside of NuSTAR's field of view. Furthermore, NuSTAR and RHESSI provide coverage in complementary energy ranges - RHESSI observes thermal emission in the 4 to ≥15 keV range while NuSTAR is dominated by counts in the 2 to 5 keV range. RHESSI is therefore necessary not only for confirmation and cross-checks of NuSTAR images and spectra, but also to greatly enhance the science that can be gained with NuSTAR.

1.2.5 Science Goal 5 – Global Structure of the Photosphere

The RHESSI solar aspect system continues to produce observations that allow us to characterize the shape and brightness of the solar photosphere at the highest levels of precision. This database is unique in several ways and represents a major contribution by RHESSI to our knowledge of solar global structure and variability, the underpinnings of the solar dynamo. To further this effort, we will continue to operate in campaign mode to obtain much larger data bandwidths during special conditions, such as RHESSI anneal operations or SDO roll maneuvers performed twice yearly when SDO gets comparable global imaging information.

During the next years, our efforts will be focused on solar cycle variations. The solar oblateness and the limb-darkening function, as well as any large-scale structures in photospheric brightness, may vary systematically with the solar cycle. Kuhn et al. (2012) have attempted a measurement of a solar-cycle dependency of the solar oblateness using SDO/AIA data but only a relatively coarse upper limit on possible variations could be supported by the observations. The RHESSI SAS data provide a more precise access to this problem. The measurement of the solar shape has proven to be more difficult around solar minimum than during solar maximum as reported by Fivian et al. (2008). For solar-minimum analysis, EUV images are used to mask regions with magnetic activity that perturb the measurement of the differential solar radius. During the last solar minimum around 2008/2009, the SOHO/EIT images used for this masking had significant limitations in spatial and temporal resolution. The upcoming solar minimum will be supported with SDO/AIA observations providing greatly improved spatial and temporal coverage compared to SOHO/EIT. Consequently, the oblateness measurements will be of much greater scientific impact than the measurements from the previous minimum. It is thus important to continue the acquisition of RHESSI SAS data through the upcoming solar minimum in order to obtain the best measure of the solar oblateness and possibly detect any variation with the solar cycle.

1.2.6 Science Goal 6 – Nonsolar Objectives

In its current configuration with two detectors typically active, RHESSI cannot detect a significant number of TGFs on its own – this is not just due to active area, but also to the need to use multiple detectors to screen out occasional impostor events produced by very small bursts of noise in individual detectors. However, even with two detectors, it is possible to decide whether a bright TGF was happening at a given moment if the specific time is provided by another observer (i.e., a TGF was detected by another spacecraft, or a radio signal very characteristic of TGFs was seen under RHESSI's footprint, or another exotic lightning-related event occurred that could be checked for high-energy radiation, like a sprite or blue jet). In this context, RHESSI's status as the only TGF-detecting instrument with inclination >28º makes it still a unique resource; it can sample storms in non-tropical regions, providing a greater variety of meteorological context and therefore a better sense of the role of TGFs in different storm types.

1.3 Potential for Performance from FY-18 through FY-22

RHESSI is directly relevant to the SMD Science Plan and for achieving NASA's strategic goal for Heliophysics to "Understand the Sun and its interactions with the Earth and the solar system." It addresses the SMD Science Question – "What causes the Sun to vary?" and the following Science Area Objectives: "Understand the fundamental physical processes of the space environment from the Sun to Earth" and "Maximize the safety and productivity of human and robotic explorers by developing the capability to predict the extreme and dynamic conditions in space."

1.3.1 Productivity and Vitality of Science Team

The first fifteen years of RHESSI operations have been extraordinarily productive. To date, RHESSI observations have contributed to ~2,000 refereed papers and over 100 PhD and master's theses listed at the following web site: http://hesperia.gsfc.nasa.gov/rhessi3/news-and-resources/results/. The annual numbers of refereed articles and citations related to RHESSI are shown in Figure 20 as obtained from the NASA ADS web site by searching for the words "HESSI" or "RHESSI" in the title, abstract, or text.

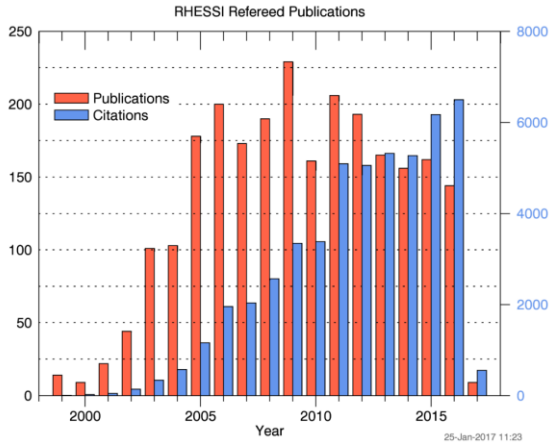

Figure 20. Number of refereed publications per year (red, left scale) that involve RHESSI and the number of citations per year to those papers (blue, right scale)

The RHESSI PI team created and supports the Max Millennium program accessible at http://solar.physics.montana.edu/max_millennium/. It serves several functions that are key to the successful acquisition of observationally complete datasets and the full scientific exploitation of those observations. These functions include the daily recommendations of targets for joint observations and the establishment of joint observing plans with specific scientific goals in the event of predicted major flare activity.

RHESSI personnel have initiated, organized, and attended many scientific meetings and special sessions, including fifteen RHESSI-specific workshops with a sixteenth planned in June 2017 in Boulder, CO. Several international teams of scientists have also met under the sponsorship of the International Space Science Institute (ISSI) to explore issues related to RHESSI science. We will continue this sequence of scientific meetings.

Beginning in March 2005, the RHESSI team began a biweekly series of "Science Nuggets" at http://sprg.ssl.berkeley.edu/~tohban/wiki/index.php/RHESSI_Science_Nuggets. Each Nugget is a brief report that is intended to introduce various aspects of the scientific material to a technically competent audience, and often include novel as-yet-unpublished insights. Both RHESSI team members and a worldwide community of interested scientists contribute to the Nuggets, now over 290 in number.

1.3.2 Data Accessibility and Usability

Full details of RHESSI data accessibility and usability are given in the accompanying Mission Archive Plan. The data archive contains the full Level-0 telemetry data, the RHESSI flare list, and quicklook lightcurves, spectra, images, and housekeeping plots for the entire mission. These plots, as well as context information discussed below, are easily accessed using the RHESSI Browser, http://sprg.ssl.berkeley.edu/~tohban/browser/. The archive, currently ~9 TB, resides on

a private server at SSL and two public servers, one at Goddard and the other at FHNW in Switzerland. Extensive RHESSI documentation is at

http://hesperia.gsfc.nasa.gov/rhessidatacenter/

with comprehensive descriptions of the mission, the instrument, the science objectives, data analysis techniques, the software, and the data archive. In addition, support personnel are available at all three data sites to guide scientists in using the software and interpreting the results.

1.3.2.1 *Software*

One of the unique characteristics of RHESSI is that the telemetered data contain detailed information on each detected photon. This provides the flexibility to make *ex post facto* decisions and tradeoffs associated with time resolution, energy resolution, imaging resolution and field of view, enabling the analyst to optimize these parameters as needed. Another advantage of this photon-oriented database is that ongoing improvements to the software and instrument calibration can be fully applied retroactively to all the data since the beginning of the mission.

The complete RHESSI software package necessary for the analysis of all RHESSI data is available online as part of the Solar Software (SSW) tree. The software generates image cubes (in time and energy), spectra (either spatially-integrated or feature-specific), and light curves, and provides support for comparisons with data products from other missions.

Spectral analysis capabilities are now enhanced by adding templates for the gamma-ray lines between ~300 keV and 10 MeV that depend on the spectrum, composition, and directionality of the accelerated ions, and the ambient solar abundance. Templates of pion-decay gamma-ray spectra extending to higher energies covered by Fermi GBM and LAT are also available.

Powerful visibility-based X-ray analysis can now be routinely carried out using several different image-reconstruction algorithms that include the capability to compute spectrally regularized image cubes. Visibilities are calibrated, instrument-independent, Fourier components of the source image. Mathematically, they correspond to the output of a single baseline of a radio interferometer. For RHESSI, they represent an intermediate data product directly obtained from the observed time-modulated light curves. The basic visibility software has enabled the accurate determination of HXR source sizes (useful for example to convert thermal emission measurements to electron densities), and the evaluation of albedo; it was the computational tool of choice in obtaining several of the recent results discussed above. The ESA-funded project, High Energy Solar Physics in Europe (HESPE http://www.hespe.eu/), has compiled a set of visibility-based data spanning the duration of the RHESSI mission, thus allowing the essential imaging spectroscopy information to be encoded very compactly.

1.3.2.2 *Facilities for Multi-Wavelength Analysis*

The following steps have been taken to support the convenient integration of RHESSI data into studies involving other wavelength regimes:

- The RHESSI software package includes flexible tools for accessing and integrating multiple data sets (e.g. overlaying images from different instruments). Coalignment is simplified since the absolute positions of RHESSI images are inherently determined to arcsecond accuracy.
- The Synoptic Data Archive at the GSFC Solar Data Analysis Center (SDAC) provides access to image, spectral, and lightcurve datasets spanning a broad wavelength range from radio to gamma-rays.
- SDO/AIA cutout image FITS files and movies generated for every RHESSI flare after September 2010 are linked from the RHESSI Browser, and the FITS files are available through the Synoptic Data Archive mentioned above.

- Science-ready RHESSI time profiles, images, and spectra conforming to SPASE guidelines are now being generated for each event. They will be accessible from the RHESSI Browser, through the VSO (and therefore the Synoptic Archive), and in (J)Helioviewer.
- The spectral analysis software package written for RHESSI also handles X-ray and gamma-ray data from Fermi/GBM and LAT, MESSENGER/SAX, and SOXS, allowing users to analyze these different data types alone or jointly with RHESSI data in a familiar environment

The RHESSI web-based Browser is available at the following location:
http://sprg.ssl.berkeley.edu/~tohban/browser/?show=grth+qlpcr
It provides a quick and easy way to display the wealth of RHESSI quicklook plots and to investigate the context of RHESSI events with data from many other instruments.

1.3.3 Promise of future impact and productivity

RHESSI is currently operating with just two of the nine germanium detectors activated. This is to reduce the heat load on the cryocooler and hence keep the detector temperature at the lowest possible level. Detectors #3 and #6 are kept activated since they cover angular resolutions of 7 and 35 arcsec (FWHM), respectively, and allow images to be reconstructed for sources extending over that range. To improve image quality, all detectors will be activated for a few days if solar activity ramps up and multiple large flares are predicted. RHESSI is expected to continue in this state for at least another two years. It continues to be the only mission capable of solar HXR imaging spectroscopy and is likely to retain that unique position until the launch of the Spectrometer Telescope for Imaging X-rays (STIX) on the European Solar Orbiter with a nominal start of science observations in 2020 with the possibility of earlier cruise-phase observations following launch in late 2018 or early 2019. Thus, it is critical that RHESSI be available for as long as possible to provide the high-energy coverage of the flares seen with the advanced instrumentation on IRIS, SDO, Hinode, STEREO, and Fermi, and the improved ground-based radio and optical observatories such as EOVSA and VLA.

The long-term prospects for the RHESSI germanium detector performance are discussed in Section 2.2.1. In summary, we expect that operations can continue well into 2019, with a possible sixth anneal sometime in 2017 or 2018, with some reduction in performance but with the core HXR imaging spectroscopy capability retained.

2 TECHNICAL AND BUDGET

RHESSI is a whole-Sun imager with high spectral and spatial resolution covering X-rays and gamma-rays in the energy range from 3 keV to 17 MeV. X-ray spectral resolutions of ~1keV (FWHM) and spatial resolutions of >~2 arcsec (FWHM) are typically achieved for all detected GOES B-class to X10-class flares. Gamma-ray spectral resolutions of >~5 keV and spatial resolutions of ~35 arcsec are achieved for the largest gamma-ray-line flares. A detailed description of the RHESSI mission, instrument, and data-analysis software is given in the first six papers of the Nov. 2002 issue of *Solar Physics* (210, pp. 3–124).

2.1 Spacecraft

RHESSI was launched on February 5, 2002, into a circular orbit with an altitude of 600 km and an inclination of 38º. The observatory continues to function very well after 15 years of operations in its present 500 x 470 km orbit. It has no expendables and all of its subsystems are fully operational. The latest semi-annual lifetime predictions made by Goddard's Flight Dynamics Support Services (Code 595) dated 30 November 2016 show that the "Mean Nominal" predicted reentry date is December 2022 and the "Early +2 Sigma" date is October 2021.

The solar array power output has declined slightly since launch, but has no difficulty fully charging the battery during each daylight period. The battery pressure and temperature have increased slightly over the past few years as expected for an aging battery with less efficient

charging and reduced capacity. To avoid the possibility of over-discharging the battery during nighttime, the load on the battery has been reduced by not having any regularly scheduled passes during nighttime. (Transmitter power during daylight passes draws from the ample solar-array power.) There is sufficient daylight coverage across all of the ground stations (including Berkeley, Wallops, and Santiago) to downlink all of the instrument data.

The average spacecraft temperature has increased by only ~1º C since launch. The S-band transceiver still generates a stable output power of 5 W with clean BPSK modulation at 4.0 Mbps, and the receiver shows no signs of deterioration in performance. The attitude control system is stable and the C&DH subsystem shows no signs of degradation. Noise in the spacecraft power bus inhibits ATS table loads during nighttime passes, but all passes are now nominally in daylight.

Aside from the described problems, all other subsystems and sensors are functioning nominally. Overall, there is no reason to believe that the spacecraft will not continue to function very well over the next several years.

2.2 Instruments

2.2.1 Spectrometer and Cryocooler

The RHESSI spectrometer and its Sunpower cryocooler continue to perform well. The cryocooler has operated nearly continuously for more than 130,000 hours. While its efficiency has declined over the 15 years, it is continuing to cool the germanium detectors with an input power of 75 watts and acceptable vibration. The detector temperature has increased from ~75 K to ~150 K but the dominant cause of degraded detector performance is radiation damage and the limitations of annealing to mitigate that damage. By controlling the cryocooler settings, we expect to maintain a temperature at no greater than 170 K for the next two years. At such temperatures, based on current detector behavior, we do not anticipate thermal leakage currents to reach the level where detector operation is compromised.

Each of RHESSI's germanium detectors are electrically divided into two segments. The front segment stops most hard X-rays below ~200 keV, and is used for X-ray science down to ~3 keV, while the rear segment registers gamma rays above ~100 keV, in particular in the nuclear-line region. The vast majority of flares observed by RHESSI are studied primarily using front-segment data; only a small fraction of M-class flares and about half of all X-class flares produce gamma-ray emission that produce useful count rates in the rear segments.

Radiation damage from encounters with radiation belt protons in the South Atlantic Anomaly gradually degrades the energy resolution of RHESSI's detectors, and, when it advances to an extreme degree, renders the outer cylindrical layer of the detector volume insensitive to interactions. This has a more significant effect on the gamma-ray performance than on the X-ray performance. Five times over the course of the mission, in November 2007, April 2010, January 2012, June 2014, and February 2016, RHESSI's germanium detectors were annealed to reverse the effects of radiation damage resulting in the recovery of the energy resolution and sensitive volume. In this procedure, the detectors are heated to ~100º C for at least a week. With each anneal, X-ray resolution and effective area are nearly fully recovered, while gamma-ray resolution and effective area are partially recovered.

Unfortunately, these periods of high temperature also blur the electrical boundary between the two segments of each detector, and a higher operating voltage may be required to obtain segmentation. A detector that is operated as unsegmented has broadened energy resolution (~10 keV FWHM at 100 keV versus 1–2 keV) and increased threshold energy (~20 keV versus 3 keV). Unsegmented detectors can nonetheless be used for RHESSI's core observational capability of imaging spectroscopy above ~20 keV with no loss in angular resolution or sensitivity to events well above background. Radiation damage over time actually reduces the voltage required to obtain segmentation, and thus mitigates this consequence of annealing. Following

the most recent anneal, four of the nine detectors were immediately capable of segmented operation, and a fifth later became segmentation capable.

Based on the history of detector degradation following the previous anneals, we may perform a sixth anneal in 2017 or 2018 if cryocooler performance allows. If we choose to no longer anneal the detectors, gamma-ray performance will not be recovered, but X-ray spectral resolution will be better or comparable to unsegmented detectors for years, albeit with reductions in effective area and corresponding losses in sensitivity. Hard X-ray imaging above 20 keV is virtually unaffected except for weak flares where sensitivity above the increased background becomes an issue.

To accommodate the reduced efficiency of the cryocooler, the nominal mode of operation is to have only two of the nine detectors operating, because each operating detector adds heat into the spectrometer. As shown in Figure 21, RHESSI's core science is still achievable even with fewer operational detectors. This figure shows data for a flare on 2016 May 24 made with only two segmented detectors turned on: #3 and #8 with FWHM angular resolutions of 7 and 106 arcsec, respectively. Using only two detectors, RHESSI's ability to make X-ray light curves, spectra, and images at multiple energies is not significantly compromised for many types of

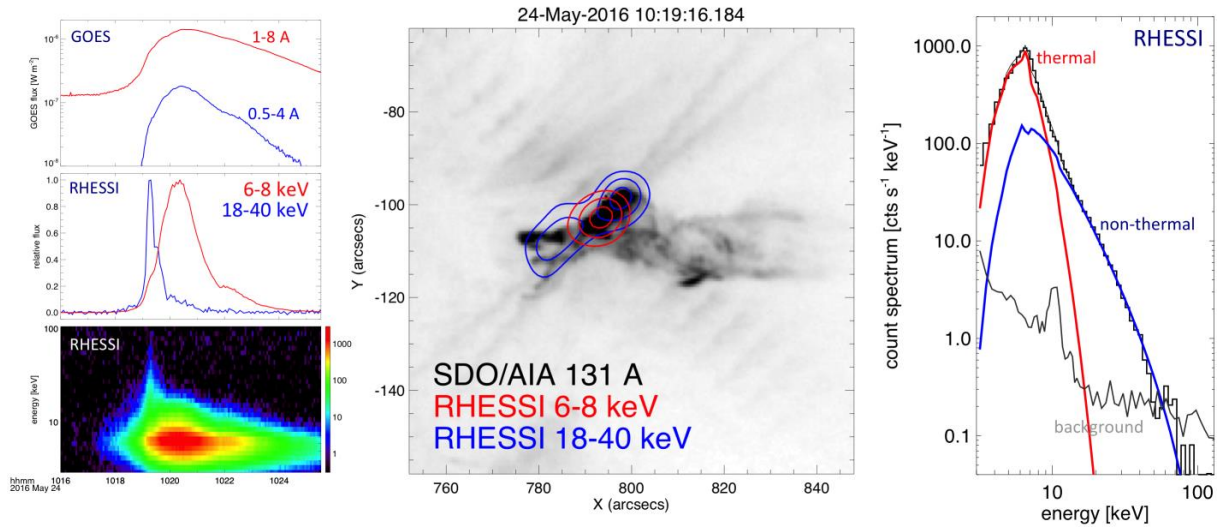

Figure 21. RHESSI observations of a GOES C1 flare on 24 May 2016 with only two detectors turned on (#3 and #8). RHESSI still provides key data products for flare studies – light curves, images, and spectra. Left: hard X-ray time profiles in the thermal (6–8 keV, red) and non-thermal (18–40 keV) energy ranges. Center: X-ray imaging showing two non-thermal foopoints (blue) and a thermal loop between them (red). Right: X-ray count-rate spectrum at the time of the peak HXR emission fitted with an isothermal component with a temperature of 15.9 MK and an EM of 1.7×10^{47} cm^{-3}, and a non-thermal component corresponding to 9×10^{27} erg s^{-1} input into the footpoints by flare-accelerated electrons with a power-law spectrum above 10 keV.

analysis. While there is a nominal ~80% reduction in overall sensitive area, the effective reduction is significantly less than this because the best spectroscopy and imaging is typically performed using data from selected individual detectors with the best energy resolution, and with angular resolutions appropriate for the dimensions of the sources under study. In the current operating mode, we expect to continue generating X-ray spectra and images for all detected events above the GOES B2 level over energies from 4 keV up to the energy (~50 keV in case shown in Figure 21) at which the solar signal falls below the non-solar background count rates.

This demonstrates that RHESSI will continue making its most important contribution in the mature phase of its mission: revealing the sites of high-energy electron interactions in flares that are studied across wavelengths by a variety of spacecraft and ground-based instruments. Imaging spectroscopy will still be possible, even with unsegmented detectors, in relatively broad

energy bands above the ~20 keV threshold. For example, energy bins of 20–30 keV and 50–70 keV could still provide cleanly separated images of superhot thermal emission and non-thermal emission in a large flare. Spatially integrated spectra will still be possible above ~20 keV so that RHESSI will still be able to provide estimates of the total energy in non-thermal electrons for input to flare models.

2.2.2 Imager

The RHESSI imager subsystem consists of nine rotating modulation collimators, each of which has a pair of widely separated grids. A metering structure maintains the relative twist alignment of the nine grid pairs. The imaging subsystem is inherently stable and has shown no evidence of change in grid alignment. Improved analysis techniques are refining the calibration of the grid parameters and locations (now known to submicron accuracy), the results of which are built into the software package and are applicable to all data acquired since launch.

2.2.3 Aspect System

There are three parts to the RHESSI aspect system. The absolute pitch and yaw angles relative to Sun center are provided by the Solar Aspect System (SAS), with sub-arcsecond accuracy. The roll angle is provided by two redundant side-looking star scanners, a CCD Roll Angle System (RAS) and a PhotoMultiplier-Tube Roll Angle System (PMT-RAS).

The SAS consists of a set of three identical lens/sensor subsystems, each of which focuses a narrow-bandwidth image of the solar disk onto a linear CCD array. No anomalies in its operation have been observed and the sensitivity is stable with an order-of-magnitude margin before there would be any compromise in accuracy. The PMT-RAS continues to provide the roll angle knowledge upon which most of the solar imaging is based. Its response has remained stable since launch, easily meeting the 1 arcminute roll-angle requirement with a large margin in sensitivity. The CCD RAS has also proven to be stable and able to meet the same roll-angle requirement. Its data are used to fill occasional gaps in the PMT-RAS coverage.

2.3 Ground System

In 1999, a multi-mission operations facility was established at SSL to support the RHESSI and FAST missions. The joint facility, which now also supports other missions, includes the Mission Operations Center (MOC), the Science Operations Center (SOC), the Flight Dynamics Center (FDC), and the Berkeley Ground Station (BGS). Backup support is provided by Wallops Island (WGS), Santiago (AGO), and the DLR ground station at Weilheim, Germany. BGS has supported more than 25,000 RHESSI passes since launch, up to 5–6 passes per day. Up to 4 passes per day are obtained via other ground stations. The average daily data volume is currently ~0.6 GB with an overall telemetry recovery efficiency of ~99%.

RHESSI normal operations comprise mission planning functions, command load generation, real-time pass supports, spacecraft state-of-health monitoring, data trending, instrument configuration, and science data recovery and archiving. Generation of all ephemeris and mission planning products is based on two-line element sets that are downloaded from the Space-Track.org web site, quality checked and archived locally in a fully automated mode. Spacecraft ATS loads are built by the Flight Operations Team (FOT) and uploaded to the spacecraft multiple times per week. Every six weeks, the spacecraft is spun up from about 14.5 rpm to its nominal spin rate of 15 rpm.

The RHESSI Science Operations Center, located at SSL, consists of a RAID server, with ~13.7 TB of data capacity, and six processors. The SOC receives RHESSI data after every ground-station contact and automatically processes them to create Level-0 data files. As of January 2017, there are ~100,000 Level-0 files containing 10 TB of data. Other automated

procedures generate quick-look data containing the RHESSI observing summary, flare list, and quick-look light curves, images, and spectra.

2.4 References

Ackermann, M. et al. 2017, ApJ, 835, 219
Alaoui, M. & Holman, G. D. 2017, in preparation
Allred, J. C. et al. 2015, ApJ, 809, 104
Aschwanden, M. J. et al. 2014, ApJ, 797, 50
—. 2015, ApJ, 802, 53
—. 2016a, ApJ, 832, 27
—. 2016b, ApJ, 831, 105
—. 2017, ApJ, 836, 17
Battaglia, M. & Kontar, E. 2013, ApJ, 779, 107
Battaglia, M. et al. 2015a, ApJ, 815, 73
—. 2015b, ApJ, 813, 113
Bellm, E. C. 2010, ApJ, 714, 881
Caspi, A. et al. 2014a, ApJ, 781, 43
—. 2014b, ApJ, 788, 31
—. 2015, ApJ, 811, L1
Chen, B. et al. 2013, ApJ, 763, L21
—. 2015, Science, 350, 11238.
Doschek, G. et al. 2015, ApJ, 813, 32
Emslie, A. G. et al. 2012, ApJ, 759, 71
Effenberger, F. et al. 2017, ApJ, 835, 124
Fivian, M. D. et al. 2008, Science, 322, 560
—. 2016. AAS/SPD meeting, 47, 12.04
—. 2017, in preparation
Gimenez de Castro, C. G. et al. 2009, A&A, 507, 433
Gjesteland, T. et al. 2017, in preparation
Glesener, L. et al. 2013, ApJ, 779, 29
—. 2017, in preparation
Grefenstette, B.W. et al. 2016, ApJ, 826, 20
Guo, J. et al. 2013, ApJ, 76, 28
Hannah, I. G. et al. 2011, Space Sci. Rev., 159, 263
—. 2016, ApJ, 820, L14
Harrison, F. A. et al. 2013, ApJ, 770, 103
Holman, G. D. 2012, ApJ, 745, 52
Holman, G. D. & Foord, A. 2015, ApJ, 804, 108
Huang, N. 2016, Res. Astron. Astrophys. 16, 177
Huppenkothen, D. et al. 2014, ApJ, 793, 129
Hurford, G. J. et al. 2003, ApJ, 595, L77
—. 2006, ApJ, 644, L93
Irbah, A. et al. 2014, ApJ, 785, 89
Kaufmann, P. et al. 2004, ApJL 603, L121
Kennedy et al. 2015, A&A, 578, A72
Kleint, L. et al. 2016, ApJ, 816, 88
Kontar, E. et al. 2015, 809, 35
Kowalski, A. F. et al. 2015, Sol. Phys. 290, 3487
Krucker, S. et al. 1999, ApJ, 519,864
—. 2013, A&A Rev., 21, 58
—. 2015, ApJ, 802, 19
—. 2017a, in preparation
—. 2017b, in preparation
Kuhn, J. R. et al. 2012, Sci., 337, 1638
Kuhar, M. et al. 2015, ApJ, 816, 6
—. 2017, ApJ, 835, 6
Landi, E. et al. 2010, ApJ, 711, 75
Leach, J. et al. 1985, Sol. Phys. 96, 331.
Lin, R. P. 1985, SolPhys, 100, 537
Marsh, A. et al. 2017, in preparation
McConnell, M. L. et al. 2004, Adv. Space Res. 34, 462.
Mewaldt, R. A. et al. 2009, ApJ, 693L, 11
Mezentsev, 2016, JGR :Atmos. 121, 8006
Motorina, G. G. & Kontar, E. P. 2015, Geomag. Aeronomy, 55, 995
Nita, G. M. et al. 2015, ApJ, 799, 236
Ostgaard et al. 2015, Geophys.Res.Lett. 42, 10937
Penn, M. et al. 2016, ApJ. 819, L30
Phillips, K. J. H. et al. 2006, ApJ, 647,1480
Rast, M. P. et al. 2008, ApJ, 673, 1209
Reep, J. W.et al. 2016a, ApJ, 818, 44
—. 2016b, ApJ, 827, 145
Reid, H. et al. 2014, A&A, 567, A85
Ripa, J. et al. 2012, ApJ, 756, 44
Rubio da Costa et al. 2016, ApJ, 827, 38
Schwartz, R. A. et al. 2015, Astro&Comp, 13, 117
Share, G. et al. 2017, in preparation
Shih, A. Y. et al. 2009, ApJ, 698L, 152
Smith, D. M. 2016, JGRA, 121, 11382
Su, Y. et al. 2011, ApJ, 731,106
Suarez-Garcia, E. et al. 2006, Sol. Phys. 239, 149
Torre, G. 2015, PhD thesis, U. Genoa
Trottet, G. et al. 2011, SolPhys, 273, 339
Varady, M., et al. 2014, A&A, 563, A51
Wang, L. et al. 2012, ApJ, 759, 69
Xu, Y. et al. 2004, ApJ, 607, L131

APPENDIX

3 RHESSI MISSION ARCHIVE PLAN

Normal RHESSI (Lin et al. 2002) operations are largely autonomous, with an almost daily command upload containing the telemetry schedule and occasional adjustments to instrument parameters. Except during detector anneals, eclipse periods, passages through the South Atlantic Anomaly, and Crab Nebula observing campaigns, RHESSI observes the full Sun continuously.

The primary science data are returned in event data packets whose contents include the time, energy and detector-segment identification for each detected photon. Aspect data are provided with sufficient time resolution that the instantaneous aspect associated with each detected event can be inferred. Monitor rates with lower time resolution are also available to provide an overview of detector performance.

Data acquisition currently averages about 0.6 GB per day and is based on a store-and-dump system using a 4 GB on-board memory. There are up to ~11 prescheduled downlink passes per day divided between the Berkeley Ground Station (BGS) and NASA Wallops Ground Station (WGS) with additional telemetry support provided by ground stations at Weilheim, Germany, and Santiago, Chile (AGO).

Because the RHESSI data is photon-based, analysts can choose the optimum time, spectral and spatial resolution and coverage best suited to his/her specific science objectives and the flare(s) in question. Such decisions can therefore be made during the analysis phase, as opposed to the implementation or operations phase of the mission. This provides a powerful degree of flexibility, the value of which has been well proven over the years. Preserving this flexibility is a primary driver for the RHESSI analysis software and data strategy.

In planning for the RHESSI Mission Archive Plan (MAP), our intent is to serve three classes of future users in addition to the RHESSI core team:

- The first is the casual user who wants easy access to standard data products (light curves, spectra and images) to serve as quantitative context information for their flare studies. From their perspective, easy access and a lack of RHESSI-centric processing are important.
- The second is the future user who wants to customize their X-ray data products, perhaps using their newly developed tools and techniques. Such users are interested in convenient access to RHESSI flare data whose calibration is at an advanced stage and that minimizes their need to understand the subtleties of the RHESSI instrument.
- The third class of user is one who wants to use RHESSI's specialized capabilities and full database in non-traditional ways. Examples of these capabilities are the solar diameter measurements, the study of terrestrial gamma-ray flashes, etc. In this case, the emphasis here is to provide the relevant data in a compact form that can be used in unanticipated ways.

3.1 RHESSI Data Archive

The current RHESSI data archive contains the full Level-0 telemetry data, the RHESSI flare list, and a number of catalog or quicklook data products (QLPs) including mission-long light curves, flare spectra and images, and summaries of housekeeping data. The full archive (~10 TB as of February 2017) resides on servers at the Space Sciences Laboratory (SSL) in Berkeley, and is automatically mirrored at GSFC and the HESSI European Data Center (HEDC) at FHNW, Windisch, Switzerland. It is online and accessible by anyone. The online archive, including metadata, quicklook products and engineering data, is updated automatically, typically within an

hour of receipt at the Mission Operations Center (MOC) at SSL, by converting the received telemetry to FITS files and adding them to the online dataset where they are available for scientific analysis.

The Level-0 data files contain the full raw telemetry data in packed time-ordered format. All of the quicklook product generation and detailed analyses of RHESSI data start with the Level-0 files. These files contain science data ('photon-tagged events' that encode the detector ID, arrival time, and energy for each detector count), monitor rates, solar aspect data and housekeeping data. Even though these files are in a standard FITS format, they are meaningful only through the RHESSI SSW software due both to the complex data packing scheme and that images must be reconstructed from the instantaneous aspect and photon arrival times. Calibration information needed to interpret these data is distributed with and accessed by the analysis software. The entire Level-0 database is currently being stored in a deep archive at the NSSDC with a latency of a few months. As of February 2017, it contains data through December 2016.

The QLPs include a flare list containing the time, duration, size, location, and other parameters and flags for the >100,000 events automatically identified in the RHESSI data. The full flare list is available in the archive (and viewable through a browser) as one large text file. In addition, monthly flare list files are stored in FITS format, as well as text files for easy direct viewing. The RHESSI software reads the FITS files, automatically merging the monthly files, and provides options for selecting analysis time intervals based on flare parameters.

The QLPs allow the RHESSI observations to be surveyed. Using the same software used for higher-level analysis, they are created automatically from the Level-0 data both as FITS files and browser-viewable image formats such as GIF, PNG, or text files.

The QLP FITS files include daily observing summary data from which analysts can quickly generate plots of light curves in 9 standard energy bands. These files also contain spacecraft ephemeris and pointing information and the modulation variance. For most flares, the QLPs also include representative spectra and images that are intended as a starting point for most analyses. (Detailed analysis of a flare is done using the Level-0 data, where the user can select the times, energies, detectors, etc. that are best suited to the scientific objectives and the event under study.) The prepared plots can be viewed directly by accessing the archive metadata directories, or more easily through the versatile RHESSI Browser at http://sprg.ssl.berkeley.edu/~tohban/browser/. This allows users to display more than 20 different products including light curves, images, spectra, monitor rates, and comparisons with the 2-channel light curves from the GOES X-Ray Spectrometer (XRS).

In addition, RHESSI housekeeping data for the entire mission are available in the archive and can be accessed at https://hesperia.gsfc.nasa.gov/hessidata/metadata/hsi_1day_sohdata/. Text files and GIF plots provide a record of the average daily values for ~100 state-of-health parameters including spacecraft bus voltages and currents, imager aspect sensor parameters, spectrometer cryocooler power and temperature, and more.

Access to the current data archive is almost transparent. Users located at a site hosting the full data archive (Goddard, Berkeley, or FHNW) share the data directories from a local file server. Remote users set a feature in the software to enable network searching and copying of files from an archive to their own computer. In either case, the software automatically determines the files needed for the selected time interval, and after either sharing or copying them, reads them and retrieves the requested data for processing.

3.2 Software

Almost all the RHESSI software package (Schwartz et al. 2002) is written in Interactive Data Language (IDL, licensed from Harris Geospatial Solutions). It contains all procedures necessary to read and unpack the FITS data files, prepare and plot light curves, reconstruct images, and

accumulate, display, and analyze spectra. Analysis procedures can be invoked from a combination of the IDL command line, user-generated scripts building on these commands, or a graphical user interface (GUI) that forms a user-friendly shell around the basic analysis routines. The software is fully compatible with Linux, Mac OS X, and Windows operating systems and is freely available as part of the Solar Software (SSW) tree.

The RHESSI data analysis software is a robust object-oriented system that allows any analyst with access to Level-0 files, calibration data, and the QLPs to generate and analyze RHESSI lightcurves, spectra, and images. Higher level capabilities include generating image cubes and movies of images at multiple time and energy intervals, background subtraction, feature-based imaging spectroscopy, and performing joint analysis of many different observations of the same events by other observatories. The software can be downloaded to any user's computer as part of the Solar Software (SSW) installation following instructions provided on the RHESSI web site. The only requirement is that the user has a license for IDL version ≥6.4 (preferably ≥8.3 to be compatible with some recent features in SSW.)

3.3 Documentation and Support

Extensive documentation describing the mission, instrumentation, analysis techniques, software, and data access can be found via a single RHESSI web site: http://hesperia.gsfc.nasa.gov/rhessi/. Support personnel at SSL and GSFC are also available to provide guidance as needed in using the software and interpreting the results.

The extensive online RHESSI documentation provides both background and explanatory material on the RHESSI mission, as well as instructions for almost every aspect of the software, from installation through use of the objects and the GUI. Detailed descriptions of every data product and warnings about misinterpreting data are available. There are 'First Steps' instructions for imaging and spectroscopy to guide users through sample GUI sessions and explanations of the use of the objects. A software FAQ is available to provide solutions to common questions or problems.

Core members of the RHESSI group share responsibility for responding promptly to software bug reports, database issues, and questions.

3.4 Plans for the RHESSI Archive

The RHESSI archive will include the data products, software, and documentation discussed above, as well as secondary databases of scientific interest and several new data products under development, all of which are described in more detail below. This section emphasizes the tasks related to adapting and enhancing those data sets to make them effective with a reduced (or eliminated) level of support from the instrument team.

3.4.1 Level-0 Data

To meet the needs of solar and non-solar analyses without compromising the full potential of the data, the Level-0 data as described in Section 3.1 will be made part of the Resident and Final Archives, along with the corresponding analysis tools and documentation.

3.4.2 Level-1 Data Products

Quicklook Products

The Level-1 data products serve the needs of those requiring a convenient overview of the data and basic X-ray data products (light curves, representative images, and spectra, etc.). The catalog data to be archived for post-mission use are identical in form and content to that described in Section 3.1.

Flare Visibility Data

As discussed above, a key driver of the RHESSI analysis approach has been to maintain the ability of the user to flexibly choose the time, spatial, and energy resolution and range that best matches their scientific objectives and events under study. To achieve this, however, it is necessary for users to start from Level-0 data and use the RHESSI-specific IDL software package. While this continues to be effective, it may become more problematic without the occasional one-on-one interaction with experienced users. For the long-term, therefore, it is desirable to identify a way by which most of the flexibility can be maintained without necessarily resorting to the Level-0 data.

Visibilities provide a natural way to accomplish this. A RHESSI visibility is a calibrated measurement of a specific Fourier component of the source spatial distribution for a given time interval and (count) energy bin. Spatially, each visibility corresponds to a single uv point (in radio parlance). Such visibilities are a direct output of RHESSI's time-modulated measurements of X-ray flux. While RHESSI's 'normal' imaging algorithms bypass the explicit calculation of visibilities, the object-oriented software to convert RHESSI's photon-based data to calibrated visibilities has been incorporated into the RHESSI software package and an increasing fraction of papers now use visibility-based analyses. Furthermore, some capabilities, such as the generation of electron-images, can only be generated through visibilities. In addition to the efforts of the RHESSI PI team, the High Energy Solar Physics in Europe (HESPE) program, funded by ESA, is generating and archiving visibility-based data for long-term use.

While making some compromises in time and/or energy resolution, the use of visibilities has several distinct advantages.

- Visibilities are an inherently compact representation of the RHESSI data, preserving its key information content in a form that is typically $\geq$2 orders of magnitude more compact than photon-based data.
- Unlike reconstructed images, visibilities are a *linear* representation of the data so they can be combined across different time/energy ranges to meet the user's needs.
- For each detected energy range, visibilities are calibrated, thus relieving the user of instrument-specific calibration tasks.
- Visibilities provide a more robust method of determining accurate source sizes as compared to inspection of reconstructed images.
- Measured visibilities include well-determined statistical errors whose propagation supports quantitative assessment of the significance of derived results.
- Currently, three of the 8 RHESSI image reconstruction algorithms are based on visibilities. Because of the simplicity of visibilities, the remaining algorithms can be readily converted to use them, and all of the algorithms can be translated to other programming languages such as Python, for more universal access.

These considerations suggest that, in addition to the catalog and Level-0 data products discussed above, the inclusion of an extensive set of calibrated flare X-ray visibility data would provide a flexible option to meet the needs of users well into the future.

To do so, the following tasks remain to be accomplished:

- While the basic software for visibility calculation has been implemented, there are several important areas in which it needs to be refined. For example, combining energy and time subsets of visibilities to larger units is currently possible, but the interface to control this task must be developed.
- Automated algorithms need to be developed to optimally choose statistically significant time and energy intervals within which to calculate visibilities. Such algorithms are

currently under development for other missions (e.g., STIX on Solar Orbiter) and can be re-parameterized for the present purpose.

- Scripts need to be developed and executed to apply these algorithms to the mission-long RHESSI data set and to convert the visibilities to the archive format.
- More extensive documentation needs to be developed for use by unsupported users in the Resident and/or Final Archive phases.

Flare Event List and Livetime Databases

While the visibility database provides a compressed representation of the RHESSI data that can be used for many types of analysis, some studies may need the more basic original RHESSI data, but in a form that can be used with tools other than our IDL software. To this end, for each flare time interval, we will write event list and livetime FITS files covering the energy range of the flare. The event list will contain the calibrated energy value in keV and the time for each count (event) in each detector segment. The livetime file will contain the 'corrected' livetime (incorporating data gaps caused by passage of high-energy particles that saturate the front-end electronics and any other contributors to dead time) for each detector segment at high time resolution (512 microseconds). Users will be able to read these files and compute RHESSI count rates in any software environment, since we will have already taken care of the difficult software issues involved in unpacking the data. The tools for extracting the event list and livetime data from the Level-0 data already exist, but would have to be tailored to create this archive.

Flare Spectrogram Database

Another useful database we plan to create is a spectrum FITS file and associated detector response FITS file for each flare time interval. Typically, these files will have 50–100 energy bins from 3–300 keV with high time resolution. These files can be used as input to our spectral analysis package in SSW (OSPEX), but would also be suitable for use with other packages in other analysis languages. The software to write these files already exists.

3.4.3 Level-2 Data Products

We are in the process of adding three science-ready flare-oriented databases for photon images, spectra and lightcurves. This effort has been funded under the data environment enhancement program. The FITS files created will be readable in any scientific software environment. For each flare, we will include:

- High quality photon flux images made using the pixon algorithm in our standard energy bands at a cadence dictated by the data rates. Using about 10,000 counts per sub-collimator, these images will show the principal flaring structures in the corona at low energy, and in the chromosphere at higher energy. While not suitable for imaging spectroscopy or high time-resolution studies, they will be extremely useful in correlative studies at non-X-ray wavelengths and will require no further RHESSI-specific analysis. Recent improvements to the pixon routine have increased its speed by a factor of 3–10.
- Photon lightcurves made in our standard energy bands up to 300 keV. These data will be background-subtracted allowing for spectral deconvolution from counts to photons. While it won't be possible to remove all instrument artifacts, these lightcurves will be suitable for immediate display and comparison with other wavelengths.
- Photon spectra up to 300 keV will be produced on a time-scale commensurate with the images produced in the non-thermal energy range. Count spectra and estimated background spectra will also be available, as well as any needed detector responses for use with our spectral analysis package, so that different model spectral forms could be used to satisfy any new science objective.

The additional databases described in this section have the common feature that the data are distributed throughout the multi-terabyte Level-0 database. For the convenience of non- experts, we will extract and process the relevant material into compact, standalone databases for subsequent analysis.

Solar Diameter Data

In addition to providing essential pitch and yaw aspect data for X-ray image reconstruction, the Solar Aspect System (SAS) data constitute a unique database of highly precise measurements of solar diameters (Fivian et al. 2005) with applications to fundamental solar properties such as solar oblateness and p-modes. The dataset comprises ~100 diameter measurements per second (totaling $>5x10^{10}$ measurements to date), each with a statistical error of a few tens of milli-arcseconds.

SAS data require elaborate analyses to remove diverse systematic effects in order to fully exploit their inherent precision. As a result, these data benefit from the creation of secondary databases, both to isolate the SAS data set itself and to reflect the application of internally derived calibration parameters. Although a preliminary version of such a database exists, for the legacy archive, it will need to be finalized and fully documented.

Roll Aspect Database

We are creating a Roll Aspect Solution database for the entire mission. Currently, the software determines the instantaneous roll solution based on the PMTRAS (Photomultiplier Roll Angle System) data that are included in the Level-0 files. We estimate that this software works successfully ~98% of the time based on the number of flare locations at implausible high latitudes and various internal checks. We want to reduce that error rate, particularly as the availability of expert assistance becomes lessened as our staffing levels decrease. Therefore, we will extract the entire set of PMTRAS data and will use that to create a robust roll solution database.

Radiation Studies

Mission-long examination of nuclear radiation data is useful for studies of galactic Al^{26}, galactic positron annihilation, novae, and quiet-Sun 2.2 MeV neutron-capture-line emission. As the mission progresses a database of accumulated 1-minute spectra from the rear detector segments is being amassed and will be added to the archive. Documentation will be generated during the transition to the Resident Archive phase.

Terrestrial Gamma-Ray Flashes (TGFs)

A catalog of transient events identified by an automated TGF triggering algorithm is being assembled as the mission progresses. During the Resident Archive phase, this will be finalized and documented for use as part of the Final Archive.

Spectrometer Status Database

We are collecting complete records of the status of the spectrometer, including detector segmentation and threshold level changes resulting from radiation damage and detector annealing. These augment the existing calibration files and will facilitate detector selection in both spectroscopy and imaging analyses that is of particular importance to non-experts.

SDO/AIA Cutout Image Database

SDO/AIA cutout image FITS files and movies are generated for every RHESSI flare observed above 12 keV after the SDO launch in February 2010. The cutouts are 400 x 300 arcsec rectangles at the highest cadence for all the AIA channels covering from a few minutes before the start of the RHESSI flare though a few minutes after the end. These movies are linked from the RHESSI Browser, and the FITS files are accessible through the Synoptic Data Archive with only a few days delay.

3.5 Analysis Tools for Level-0 data

The basis for all legacy archive analysis tools is the IDL-based, SSW-distributed software that has been routinely used during the mission for the creation and interpretation of scientific data products. To maintain the integrity of the software within the dynamic SSW environment we will archive a snapshot of all the elements of the SSW tree necessary for RHESSI analysis, specifically the GEN, HESSI, X-RAY, and SPEX branches. This will ensure that the software that was working at the end of mission will continue to work into the future. Additionally, we will build web-based form scripts that can be used remotely or through a data tech at the SDAC to allow building our enhanced data products for users without access to IDL.

With successive cycles of progressive radiation damage and annealing, the RHESSI detector response has changed during the course of the mission. To accommodate this, detector response parameters in the SSW distribution have been periodically updated so that, transparent to the user, the appropriate time-dependent calibration parameters are applied for each analysis. In preparation of the legacy archive, it will be necessary to ensure that this calibration has been updated as required to cover the full mission.

3.6 Documentation

While an extensive range of documentation is available via the RHESSI website, it needs to be carefully reviewed so that it can effectively serve its purpose, both during the Resident Archive phase when RHESSI personnel will still be available and during the Final Archive phase with reduced (or absent) one-on-one support. Specifically, obsolete or conflicting material needs to be identified and updated or removed, perceived gaps need to be identified and a robust stand-alone guide to the material generated. While on-going at a low level, this task will be completed during the Resident Archive phase, requiring an estimated 2–4 months of effort by a combination of experienced RHESSI personnel. Particular emphasis will be placed on introductory material, indexing, and consolidating distributed information to provide a mission-long overview and time-ordered log of RHESSI performance.

3.7 Distribution

For several years after the end of the mission, RHESSI data products will continue to be accessible from servers at SSL, GSFC, and possibly through the Swiss-funded mirror site at FHNW. The archive will then be transitioned to the Solar Data Analysis Center (SDAC) at Goddard, with the Final Archive hosted by the National Space Science Data Center (NSSDC) also at Goddard.

To provide access to archived RHESSI data products through the VSO, we will:

- Make it possible to display the quicklook data products, and later, the science ready images and spectra in VSO query results and download pre-calculated images, image cubes, or spectra for comparison with data sets from other instruments.
- Implement event-based queries, e.g., searches for flares with specific characteristics such as size, duration, or location.
- Provide an indexed database of flare visibilities so that a subset of visibilities based on user-requested time and energy can be extracted and returned to the user.
- Include SPASE keywords in the headers to our FITS files to guarantee that SPASE data analysis programs can use the RHESSI data.

We are also investigating uploading the RHESSI metadata to the Heliophysics Events Registry (HER) for use through the Heliophysics Events Knowledgebase (HEK), and by extension Helioviewer and other web-based tools for searching and displaying solar data.

3.8 IDL Alternatives

While IDL remains the analysis programming language of choice for most solar physics missions many scientists are turning to alternatives such as Python under SunPy. Python offers many cost-saving advantages and is more widely used than IDL for tasks outside of data analysis. It would be a monumental task to rewrite the entire RHESSI IDL software package in another language, but by providing the legacy databases listed above, many science tasks can be accomplished in Python. The FITS files in the RHESSI legacy archive can easily be read with PyFITS readers. Spectral analysis tools have already been written in Python (e.g., Sherpa and PyXspec) although specialized photon models would have to be implemented for solar analysis. In addition, most of our visibility imaging algorithms can be implemented with Python in a straightforward way. We will provide Python routines for the Clean, Pixon, and ForwardFit image reconstruction algorithms as part of the legacy archive tools. (Clean and Pixon routines based on visibilities have not yet been written in IDL, but are in progress after the recent realization that the difference between our current input format of the stacked calibrated event lists and visibilities are minor.)

3.9 References

Fivian, M. D., Hudson, H. S., & Lin., R. P. 2005 in *Proc 11th European Solar Physics Meeting*, ESA SP- 600, 41

Lin, R. P., et al. 2002, Solar Phys., 210, 3

Schwartz, R. A., et al. 2002, Solar Phys., 210, 165

ACRONYM LIST

A&A	Astronomy & Astrophysics Journal
AAS	American Astronomical Society
ACE	Advanced Composition Explorer
ADS	SAO/NASA Astrophysical Data System (adsabs.harvard.edu)
AGO	Santiago ground station
AGU	American Geophysical Union
AIA	Atmospheric Imaging Assembly on SDO
AIM	Aeronomy of Ice in the Mesosphere
ALMA	Atacama Large Millimeter/submillimeter Array
ApJ	Astrophysical Journal
AR	Active Region
ATS	Absolute Time Sequence
AU	Astronomical Unit
BGS	Berkeley Ground Station
BPSK	Binary Phase Shift Keying
CCD	Charge Coupled Device
C&DH	Command and Data Handling
CME	Coronal Mass Ejection
COSPAR	COmmittee on SPAce Research
DEM	Differential Emission Measure
DKIST	Daniel K. Inouye Solar Telescope (formerly the Advanced Technology Solar Telescope, ATST)
DLR	Weilheim ground station
EIT	Extreme Ultraviolet Imaging Telescope on SOHO
EIS	EUV imaging spectrograph on Hinode
EM	Emission Measure
ENA	Energetic Neutral Atom
EOVSA	Expanded Owens Valley Solar Array
ESA	European Space Agency
EUV	Extreme UltraViolet
EVE	Extreme Ultraviolet Variability Experiment on SDO
FAST	Fast Auroral SnapshoT
FAQ	Frequently Asked Questions
FDC	Flight Dynamics Center
Fermi	Fermi Gamma-ray Space Telescope (formerly GLAST)
FHNW	Fachhochschule Nordwestschweiz - University of Applied Sciences and Arts, Northwestern Switzerland
FIP	First Ionization Potential
FITS	Flexible Image Transport System
FOT	Flight Operations Team
FTE	Full time Equivalent
FWHM	Full Width at Half Maximum
GB	Gigabytes
GBM	Gamma-ray Burst Monitor on Fermi
GIF	Graphics Interchange Format
GLAST	Gamma-ray Large Area Space Telescope (now Fermi)
GOES	Geostationary Operational Environmental Satellite
GRB	Gamma Ray Burst
GREGOR	Gregory-type German 1.5 m solar telescope on Tenerife
GRIS	GREGOR Infrared Spectrograph
GSFC	Goddard Space Flight Center
GUI	Graphical User Interface
HEDC	HESSI European Data Center
HEK	Heliophysics Events Knowledgebase

HER	Heliophysics Events Registry
HESPE	High Energy Solar Physics in Europe
HESSI	High Energy Solar Spectroscopic Imager (now RHESSI)
Hinode	Japanese solar satellite (formerly Solar-B)
HMI	Helioseismic and Magnetic Imager on SDO
HSO	Heliophysics System Observatory
HXR	Hard X-ray
IBIS	Interferometric BIdimensional Spectropolarimeter (installed at Dunn Solar Telescope)
IDL	Interactive Data Language
IPN	Interplanetary Network
IR	Infrared
IRIS	Interface Region Imaging Spectrograph (SMEX mission)
ISSI	International Space Science Institute
ITOS	Integrated Test and Operations System
JGR	Journal of Geophysical Research
LAT	Large Area Telescope on Fermi
LDGRF	Long Duration Gamma-Ray Flares
MAP	Mission Archive Plan
MB	Megabytes
MESSENGER	MErcury Surface, Space ENvironment, GEochemistry, and Ranging
MinXSS	Miniature X-ray Solar Spectrometer (CubeSat)
MK	Megakelvin
MOC	Mission Operations Center
MO&DA	Mission Operations and Data Analysis
NASA	National Aeronautics and Space Administration
NEN	Near Earth Network
NOAA	National Oceanic and Atmospheric Administration
NSO	National Solar Observatory
NSSDC	National Space Science Data Center
NuSTAR	Nuclear Spectroscopic Telescope Array (astrophysics SMEX mission)
OSPEX	Object Spectral Executive (SSW analysis package)
PICARD	PICARD (ESA mission)
PMTRAS	Photomultiplier Tube Roll Angle System on RHESSI
PNG	Portable Network Graphics
POLAR	Compton polarimeter on Tiangong 2
PSG	Prioritized Science Goal
QLP	Quick Look data Product
RAID	Redundant Array of Inexpensive Disks
RAS	Roll Angle System on RHESSI
RHESSI	Reuven Ramaty High Energy Solar Spectroscopic Imager
SAS	Solar Aspect System on RHESSI
SAX	Solar Assembly for X-rays on MESSENGER
SDAC	Solar Data Analysis Center
SDO	Solar Dynamics Observatory
SEE	Solar Eruptive Event
SEP	Solar Energetic Particles
SGR	Soft Gamma Repeater
SMD	Science Mission Directorate
SMEX	NASA's Small Explorer Program
SOC	Science Operations Center
SOHO	Solar and Heliophysics Observatory
SOXS	Solar X-ray Spectrometer
SPASE	Space Physics Archive Search and Extract
SPD	Solar Physics Division
SPP	Solar Probe Plus
SSL	Space Sciences Laboratory (University of California, Berkeley)

SSMO	Space Science Mission Operations
SSW	SolarSoftWare
STEREO	Solar TErrestrial RElations Observatory
STIX	Spectrometer Telescope for Imaging X-rays on Solar Orbiter
SXR	Soft X-ray
TB	Terabytes
TGF	Terrestrial Gamma-ray Flash
UCB	University of California, Berkeley
UT	Universal Time
UV	Ultraviolet
VLA	Very Large Array
VSO	Virtual Solar Observatory
WGS	Wallops Ground Station
WIND	Spacecraft for long-term solar wind measurements
WL	White-Light
WYE	Work Year Equivalent
XRS	X-Ray Spectrometer on GOES